J. Fluid Mech. (1993), *vol.* 252, *pp.* 449–478

Tollmien–Schlichting-wave resonant mechanism for subharmonic-type transition

By M. B. ZELMAN AND I. I. MASLENNIKOVA
Institute of Theoretical and Applied Mechanics, Russian Academy of Sciences, 630090, Novosibirsk, Russia

(Received 4 November 1991 and in revised form 8 January 1993)

Disturbance interactions in wave triads and multiwave systems of various configurations are investigated to reveal the mechanism of laminar–turbulent transition in Blasius and pressure-gradient boundary layers. The averaging method of weakly nonlinear instability theory in quasi-parallel flows is applied. Tollmien–Schlichting-wave resonant interaction is shown to be the only leading mechanism of subharmonic (S)-type transition. The mechanism universally dominates in boundary layers excited by sufficiently small initial disturbances. The role of any other mode is inefficient. Weakly nonlinear models are concluded not to explain the K-type transition scenario. The results of the study are employed to interpret physical and numerical experimental data.

1. Introduction

The problem of transition to turbulence in boundary layers is of great fundamental and practical interest in aerohydrodynamics. The scenario for laminar–turbulent transition depends on flow type and on excitation conditions (Saric, Kozlov & Levchenko 1984; Morkovin & Reshotko 1989), and is characterized by a sequence of dominant spectral and spatial field structures. Such behaviour is obviously determined by mechanisms which are selected through the competition between interactions of disturbances of different scales. Modelling of the dominant mechanisms plays an important part in the development of laminar–turbulent transition theory, and is the main subject of the present investigation.

A number of laminar–turbulent transition scenarios have been established in a flat-plate boundary layer. In experiments by Klebanoff & Tidstrom (1959) and Klebanoff, Tidstrom & Sargent (1962), K-type transition has been established. It is characterized by intense generation of high-frequency harmonics, periodic Λ-structures of the spatial flow field, and the appearance of 'spikes' and 'breakdown' (Kachanov *et al.* 1984). Attempts were made (Benney & Lin 1960; Stuart 1962; Benney 1962) to model the K-régime by the evolution of nonlinearly interacting Tollmien–Schlichting (TS) waves which form a symmetrical non-resonant triad (figure 1*a*). Such a triad (we shall refer to it as a Benney–Lin (BL) triad) comprises a two-dimensional wave with frequency $\omega = \omega_1$ and wave vector $\boldsymbol{k}_1 = (\alpha_1, 0)$ and two oblique waves with almost equal frequencies and phase velocities: $\omega_2 = \omega_3 \approx \omega_1$, $\boldsymbol{k}_2(\alpha, \beta)$, $\boldsymbol{k}_3(\alpha, -\beta)$, $\alpha \approx \alpha_1$. The results achieved agreed qualitatively with experimental data. In particular, they described the longitudinal vortices inherent in the K-transition. Nevertheless, the problem of the mechanism responsible for the occurrence of three-dimensional periodic disturbances was still open. A likely explanation was suggested by Craik (1971, 1980). The appearance of an additional two-dimensional wave, with double the fundamental frequency, $\omega_4 = 2\omega_1$, and wave vector $\boldsymbol{k}_4 = (2\alpha, 0)$, was proposed. This two-dimensional

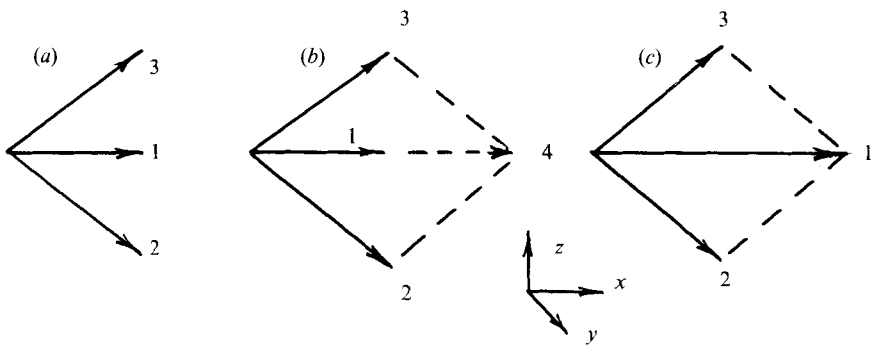

FIGURE 1. Wave vector diagrams for: (*a*) a BL-triad; (*b*) the CNB-model; (*c*) a subharmonic triad.

wave formed a symmetrical resonant triad with a pair of oblique waves with wave vectors $\boldsymbol{k}_2, \boldsymbol{k}_3$ (figure 1 *b*). Conditions of phase synchronism (resonance): $\omega_4 = \omega_2 + \omega_3$, $\boldsymbol{k}_4 = \boldsymbol{k}_2 + \boldsymbol{k}_3$, led, according to Craik, to the selection of well-defined directions of the three-dimensional wave vectors. The full system of four waves in this model ($\omega_j, j = 1, 2, 3, 4$) (we refer to it as the Craik–Nayfeh–Bozatli (CNB) model) was considered by Nayfeh & Bozatli (1979) and was analysed by Zelman & Maslennikova (1984, 1989). It must be noted that the occurrence of three-dimensionality in the K-régime may be explained as a spontaneous development of spanwise inhomogeneity of the main flow or of the initial pulsation field (Volodin & Zelman 1981; Itoh 1987; Singer, Reed & Ferziger 1989). The efficiency of the CNB-model in explaining K-breakdown needs further investigation (see §5).

A qualitatively different route to transition was observed in controlled experiments (Kachanov, Kozlov & Levchenko 1977; Thomas & Saric 1981; Kachanov & Levchenko 1982) at low amplitudes of the primary wave. The process was characterized by the preferential growth of low-frequency pulsations, a broad peak at half the fundamental frequency in the power spectrum, a staggered structure of the spatial flow field, and no 'breakdown' (Saric, Kozlov & Levchenko 1984; Kachanov & Levchenko 1984; Corke & Mangano 1987, 1989). This transition is known as the subharmonic (S) route to transition. Volodin & Zelman (1978, 1981) suggested that the formation of the S-régime could be explained by the resonant interaction (Raetz 1959; Kelly 1967; Craik 1971, 1985) of the induced two-dimensional wave with a pair of background three-dimensional TS-subharmonics which formed a symmetrical triad of Craik type (figure 1 *c*). That interaction occurred at the first nonlinear order of nonlinear stability theory and, in accordance with observations, gave rise to the rapid parametric amplification of subharmonics and, further, to explosive growth of all triad components. It was established later (Maslennikova & Zelman 1985; Zelman & Maslennikova 1984, 1989) that exact phase synchronization (C-triad) was not a necessary requirement for the maximum amplification of subharmonics. Similar conclusions, based on nonlinear asymptotic theory for large Reynolds numbers, were drawn by Smith & Stewart (1987).

Detailed experiments and numerical simulations (Corke & Mangano 1987; Saric & Thomas 1984; Zelman & Maslennikova 1984, 1989; Herbert 1988; Spalart & Yang 1987) revealed a link between the propagation angle of the selected subharmonics and the induced two-dimensional wave amplitude. This dependence was fully consistent with results based on the secondary instability method (Orszag & Patera 1983; Nayfeh 1987; Herbert 1988), although the use of this method in the region where primary and

secondary wave amplitudes are of the same order may be only formal. Because of speculation that resonant amplification of the TS-wave triad was restricted by the requirement of exact resonance, the triad model comprising three-dimensional TS-waves (Zelman & Maslennikova 1984) has been called into question (Herbert 1983, 1984; Saric & Thomas 1984), and a link between the observed subharmonics and the amplification of Squire modes (H-mechanism) was suggested. Two distinct mechanisms were supposed to operate at the S-transition: C, which was responsible for the TS-wave amplification in a narrow band of wavenumbers (exact phase synchronism in the C-triad) at low two-dimensional amplitude levels, and H, which was applicable in a wide spectral band. Questions about the nature of waves which form the dominant triad and about corresponding mechanisms were discussed in Saric & Thomas (1984), Smith & Stewart (1987), Nayfeh (1987), Zelman & Maslennikova (1989), Zelman (1989), and are still likely to be of great value for understanding the S-transition.

In the framework of the isolated triad model, neither the conditions for its appearance nor the spectrum transformation playing a direct role in the transition to turbulence can be analysed. The effects of interactions between a broad spectrum of disturbances must be taken into account. If this is the case, the initial distribution of pulsations comes into play. Its influence on laminar–turbulent transition and, in particular, on the selection of the dominant structure is another problem for theory.

In the present investigation we focus on an analysis of the weakly nonlinear mechanism of resonant interactions and their role in S-transition in boundary layers.

In §2 we formulate the problem of weakly nonlinear evolution of wave disturbances and present the method for its solution. In §3 the formation and evolution of isolated symmetric triads in boundary layers with and without pressure gradients are investigated. The mechanism of S-transition and the nature of excited subharmonics are discussed. In §4 non-symmetric triads and multiwave systems are considered, to model a mechanism for spectral broadening in S-transition. In §5 the models of K-breakdown are analysed. In the Conclusions the main results are discussed.

2. Method

The principal idea of the methods of weakly nonlinear stability theory has been formulated in the pioneering studies of Stuart (1960) and Watson (1960), and developed in many works, for example in Itoh (1974), Usher & Craik (1975). An application of the averaging method to weakly nonlinear theory suggested by Zelman (1974) is presented here.

We consider a perturbed boundary-layer velocity field

$$\boldsymbol{u} = U_\infty(U(x,y)+\epsilon \boldsymbol{V}(x,y,z,t)), \tag{2.1}$$

where $U=(U,U_1,0)$ and $\epsilon V=\epsilon(u,v,w)$ correspond, respectively, to the (x,y,z) components of the main flow; the disturbance intensity is $\epsilon \ll 1$, and $u\to(U_\infty,0,0)$ as $y\to\infty$. Equations for the normal velocity (v) and vorticity (η) components follow from the Navier–Stokes system, and in the locally parallel approximation after standard non-dimensionalization (using the free-stream velocity U_∞ and thickness $(\nu x/U_\infty)^{\frac{1}{2}}$) are as follows:

$$L^{(1)}(\eta) \equiv \left(\frac{\partial}{\partial t}+U\frac{\partial}{\partial x}-\frac{\Delta}{Re}\right)\eta = -\frac{\partial U}{\partial y}\frac{\partial v}{\partial z}+\epsilon H^{(1)}, \tag{2.2}$$

$$L(v) \equiv L^{(1)}(\Delta v)-\frac{\partial^2 U}{\partial y^2}\frac{\partial v}{\partial x} = \epsilon H, \tag{2.3}$$

$$v=\partial v/\partial y=\eta=0 \quad (y=0), \qquad (v,\partial v/\partial y,\eta)<\infty \quad (y\to\infty),$$

$$(v,\eta)=(v_0,\eta_0)\quad (t=0),\qquad \int_{-\infty}^{\infty}\mathrm{d}x\int_{-\infty}^{\infty}\mathrm{d}z\int_0^{\infty}\mathrm{d}y(|v_0|^2,|\eta_0|^2)<\infty,$$

$$\left(\frac{\partial^2}{\partial x^2}+\frac{\partial^2}{\partial z^2}\right)\begin{pmatrix}u\\w\end{pmatrix}=\begin{pmatrix}\partial/\partial z & -\partial/\partial x\\ -\partial/\partial x & -\partial/\partial z\end{pmatrix}\begin{pmatrix}\eta\\ \partial v/\partial y\end{pmatrix},\tag{2.4}$$

$$H=(\partial^2/\partial x^2+\partial^2/\partial z^2)Mv-\frac{\partial^2}{\partial x\,\partial y}Mu-\frac{\partial^2}{\partial z\,\partial y}Mw,$$

$$H^{(1)}=\frac{\partial}{\partial z}Mu-\frac{\partial}{\partial x}Mw,$$

$$M=u\frac{\partial}{\partial x}+v\frac{\partial}{\partial y}+w\frac{\partial}{\partial z},\quad \Delta=\frac{\partial^2}{\partial x^2}+\frac{\partial^2}{\partial y^2}+\frac{\partial^2}{\partial z^2}.$$

Nonlinear perturbations are assumed to originate from the evolution of infinitesimal small-scale pulsations for $t<0$, which are defined from solutions of (2.2) and (2.3) subject to $\epsilon\to 0$, and may be regarded as a series of narrow spectral wave packets:

$$\Phi=(v,\eta)=\sum_r\int_{\alpha_0}^{\infty}\mathrm{d}\alpha\int_{\beta_0}^{\infty}\mathrm{d}\beta\,A^{(r)}(\boldsymbol{k},t)\,\hat{\Phi}^{(r)}(\boldsymbol{k},y)\,\mathrm{e}^{\mathrm{i}\theta^{(r)}}$$

$$\approx\sum_{r,m}\int_{\alpha_m-\Delta\alpha}^{\alpha_m+\Delta\alpha}\mathrm{d}\alpha\int_{\beta_m-\Delta\beta}^{\beta_m+\Delta\beta}\mathrm{d}\beta\,A^{(r)}\hat{\Phi}^{(r)}\,\mathrm{e}^{\mathrm{i}\theta^{(r)}}=\sum_{l=(rm)}A_l\,\mathrm{e}^{\mathrm{i}\theta_l}\Phi_{l0}(y),\tag{2.5}$$

$$A_l=a_l(\mu x,\mu z,\mu t)\,\mathrm{e}^{\gamma_l(k)\,t},\quad \theta^{(r)}=\int\alpha\,\mathrm{d}x+\beta z-\omega(\boldsymbol{k})\,t,$$

where

$$\boldsymbol{k}=(\alpha,\beta)\geqslant(\alpha_0,\beta_0)\gg\epsilon,\quad (\hat{\Phi}^{(r)}=(\hat{v},\hat{\eta})^{(r)},\quad \omega^{(r)}+\mathrm{i}\gamma^{(r)}=\tilde{\omega}^{(r)}(\boldsymbol{k}))$$

can be evaluated from linearized theory (if $\hat{v}^{(r)}\not\equiv 0$, then $\hat{v}^{(r)}$ is an Orr–Sommerfeld (OS) eigensolution and $\hat{\eta}^{(r)}$ follows from the inhomogeneous equation (2.2); if $\hat{v}^{(r)}\equiv 0$, then $\hat{\eta}^{(r)}$ is an eigensolution of the Squire problem (2.2)); $\mu\sim|\Delta\boldsymbol{k}/\boldsymbol{k}_m|\ll 1$ characterizes the packet width, with central wave vector $\boldsymbol{k}_m=(\alpha_m,\beta_m)$; (r,l) denote the mode number and wave packet, respectively. Function $\hat{\Phi}^{(r)}$ is assumed to be independent of $\boldsymbol{k}$ within the interval $\boldsymbol{k}_m-\Delta\boldsymbol{k}\leqslant\boldsymbol{k}\leqslant\boldsymbol{k}_m+\Delta\boldsymbol{k}$. In the case of the broadband perturbation with $\mu\sim 1$, the rate of spectrum transformation, proportional to $\partial(A\hat{\Phi})^{(r)}/\partial\boldsymbol{k}$, must be taken into account (Zelman 1989).

A correct definition of the nonlinear initial value problem requires a self-consistent assignment of all harmonics at $t=0$. Our method permits us to overcome this difficulty through consideration of 'prehistory', and to transform the problem into an analysis of the nonlinear interaction of wave packets comprising eigensolutions (2.5).

The main idea of weakly nonlinear stability theory is based on the assumption that for finite perturbations $0<\epsilon\ll 1$, a pulsation field is locally similar to the linear field and that the nonlinear distortions become significant only over large scales $(x,z,t)\geqslant(\epsilon\alpha_0,\epsilon\beta_0,\epsilon\omega_0)^{-1}$, where $(\alpha_0,\beta_0,\omega_0)=O(1)$ are typical parameters. Therefore nonlinearity may enter into competition only for waves with $(|\gamma_l/\omega_l|,\mu)\leqslant\epsilon$. Then, without loss of generality, we assume $|\gamma_l/\omega_l|\sim\mu\sim\epsilon$, and seek the nonlinear solution of (2.2), (2.3) in the form

$$\Phi=\sum_s f_s\,\mathrm{e}^{\mathrm{i}\theta_s}=\sum_{N=0}\sum_s\epsilon^N f_{sN}(y,\epsilon x,\epsilon z,\epsilon t)\,\mathrm{e}^{\mathrm{i}\theta_s(x,z,t)},\tag{2.6}$$

$$f_{s0}=A_l(\epsilon x,\epsilon z,\epsilon t)\,\Phi_{l0}(y)\,\delta(s,l),\quad \frac{\mathrm{d}A_l}{\mathrm{d}t}-\gamma_l A_l=\sum_{N=1}\epsilon^N F_{lN}.\tag{2.7}$$

Here $F_{lN}, f_{sN} = (v_{sN}, \eta_{sN})$ are operators and functions to be defined; θ_s are phases, for some of which (for example, $s = l)\, \boldsymbol{k}_s$ and $\omega_s = \omega(\boldsymbol{k}_s)$ are linked by the dispersion relation of the linear problem; and δ is the Kroneker symbol.

Then we substitute (2.6) into (2.2), (2.3) and average with respect to the small-scale variables (X, Z, T), where $\epsilon^{-1} \gg (\alpha_0 X, \beta_0 Z, \omega_0 T) \gg 1$. Equation (2.3) yields

$$\frac{1}{XZT}\int_x^{x+X} \mathrm{d}x \int_z^{z+Z} \mathrm{d}z \int_t^{t+T} \mathrm{d}t\, \mathrm{e}^{\mathrm{i}\theta_s}\{Lv - \epsilon H\} = \hat{L}\left(\frac{\partial}{\partial x}+\mathrm{i}\alpha_s, \frac{\partial}{\partial z}+\mathrm{i}\beta_s, \frac{\partial}{\partial t}+\mathrm{i}\omega_s\right) v_s$$

$$-\epsilon h_{s,\,p+q}\, \hat{H}\left(\frac{\partial}{\partial x}+\mathrm{i}\alpha_p, \frac{\partial}{\partial z}+\mathrm{i}\beta_p, \frac{\partial}{\partial x}+\mathrm{i}\alpha_q, \frac{\partial}{\partial z}+\mathrm{i}\beta_q, f_p, f_q\right)$$

$$= \hat{L}_s(\alpha, \beta, \omega)\, v_s + \frac{\partial L_s(\alpha, \beta, \omega)}{\partial(-\mathrm{i}\omega)} v_s$$

$$+ \sum_{\{n_i\}} \left[\sum_{n_0=0} \hat{L}_s(n_0, \{n_i\}, v_s) - \epsilon h_{s,\,p+q} \sum_{\{m_i\}} H_{pq}(\{n_i\}, \{m_i\}, f_p, f_q) \right] = 0, \tag{2.8}$$

where the following designations are introduced:

$$\hat{L}_s(n_0, \{n_i\}, v_s) = L\left(\omega_s, \frac{\partial^{n_0+n_3+n_4} v_s}{\partial t^{n_0} \partial x^{n_3} \partial z^{n_4}}\right) \delta\left(\sum_{l=1}^{4} n_i, 0\right), \tag{2.9a}$$

$$\hat{H}_{pq}(\{n_i\}, \{m_i\}, f_p, f_q) = \hat{H}\left(\frac{\partial^{n_3+n_4} f_p}{\partial x^{n_3} \partial z^{n_4}}, \frac{\partial^{m_3+m_4} f_q}{\partial x^{m_3} \partial z^{m_4}}\right). \tag{2.9b}$$

The sums $$\left(\sum_{\{n_i\}} = \sum_{n_1=0}^{4} \sum_{n_2=0}^{4} \sum_{n_3=0}^{4} \sum_{n_4=0}^{4}\right)$$

must be carried out over all $\{m_i\}$, $\{n_i\}$, $(i = 1, 2, 3, 4)$, which take values $(m_i, n_i) = (0, \ldots, 4)$.

Also,

$$h_{s,\,p+q} = \frac{1}{XZT}\int_x^{x+X} \mathrm{d}x \int_z^{z+Z} \mathrm{d}z \int_t^{t+T} \mathrm{d}t\, \mathrm{e}^{\mathrm{i}(\theta_p+\theta_q-\theta_s)}, \tag{2.10a}$$

$$h_{s,\,p+q} = 0 \quad \text{if} \quad (\Delta\omega = \omega_s - \omega_p - \omega_q, \quad \Delta k = k_s - k_p - k_q) \gg \epsilon, \tag{2.10b}$$

$$h_{s,\,p+q} = \mathrm{e}^{-\Delta\omega t + \Delta(\alpha,\beta)(x,z)} \quad \text{if} \quad (\Delta\omega, \Delta k) \leqslant \epsilon, \tag{2.10c}$$

represents an averaging coefficient.

Derivatives in operators $\hat{L}, \hat{H}$ act with respect to 'slow' variables that raise the ϵ-order of corresponding terms. Then, for $\theta_s \neq \theta_l$, equating like powers of ϵ^N, we have for v_{sN}:

$$L_s(\alpha, \beta, \omega)\, v_{sN} = \frac{\partial L_s(\alpha, \beta, \omega)\, v_{s,\,N-1}}{\partial(\mathrm{i}\omega)} + Q_{sN}, \tag{2.11a}$$

$$Q_{sN} = -\sum_{m=0}^{\infty} \sum_{\{n_i\}} \left\{ \sum_{n_0=0}^{1} \hat{L}_s(n_0, \{n_i\}, v_{sm})\, \delta\left(N, n_0 + m + \sum_{i=1}^{4} n_i\right) \right\}$$

$$- h_{s,\,p+q} \sum_{k=0} \sum_{\{m_i\}} \hat{H}_{pq}(\{n_i\}, \{m_i\}, f_{pm}, f_{qk})\, \delta\left(N, m + k + 1 + \sum_{i=1}^{4} (m_i + n_i)\right). \tag{2.11b}$$

Correspondingly, for the definition of η_{sN} we have (with $' \equiv \mathrm{d}/\mathrm{d}y$):

$$L_s^{(1)}(\alpha,\beta,\omega)\,\eta_{sN} = -U'\mathrm{i}\beta_s v^{sN} - U'\frac{\partial v_{s,N-1}}{\partial z}$$
$$-\frac{\partial \eta_{s,N-1}}{\partial t} + U\frac{\partial \eta_{s,N-1}}{\partial x} - \frac{\mathrm{i}\alpha_s}{Re}\frac{\partial \eta_{s,N-1}}{\partial x}$$
$$-\frac{1}{Re}\frac{\partial^2 \eta_{s,N-2}}{\partial x^2} - \frac{\mathrm{i}\beta_s}{Re}\frac{\partial \eta_{s,N-1}}{\partial z} - \frac{1}{Re}\frac{\partial^2 \eta_{s,N-2}}{\partial z^2}$$
$$+\sum_{k,m}\sum_{\{n_i\}}\sum_{\{m_i\}} H_{pq}^{(1)}(\{n_i\},\{m_i\},f_{pm},f_{kq})\,\delta\Big(N, m+k+1+\sum_{i=1}^{4}(m_i+n_i)\Big). \tag{2.12}$$

For $\theta_s = \theta_l$ (where k_l and ω_l correspond via the linear dispersion relation), $L_l(\alpha,\beta,\omega)$ differs from the OS-operator $L_l(\alpha,\beta,\omega+\mathrm{i}\gamma)$ by next ϵ-order quantities with value $|\gamma_l/\omega_l| \sim \epsilon$. Without loss of accuracy we make the substitution $f_l = \tilde{f}_l\,\mathrm{e}^{\gamma_l t}$ and separate the OS-operator in the explicit form:

$$L_l(\alpha,\beta,\omega)\,v_l + \frac{\partial L_l(\alpha,\beta,\omega)}{\partial(-\mathrm{i}\omega)}\frac{\partial v_l}{\partial t} = \mathrm{e}^{\gamma_l t}\Big(L_l(\alpha,\beta,\omega+\mathrm{i}\gamma)\,\tilde{v}_l + \frac{\partial L_l(\alpha,\beta,\omega)}{\partial(-\mathrm{i}\omega)}\frac{\partial \tilde{v}_l}{\partial t}\Big). \tag{2.13}$$

Then
$$L_l(\alpha,\beta,\omega+\mathrm{i}\gamma)\,\tilde{v}_l = \frac{\partial L_l(\alpha,\beta,\omega)}{\partial(\mathrm{i}\omega)}\frac{\partial \tilde{v}_l}{\partial t} + \sum_{N=1}\epsilon^N Q_{lN}\,\mathrm{e}^{-\gamma_l t},$$

and taking into account (2.7) we have for $\tilde{v}_{lN}$:

$$L_l(\alpha,\beta,\omega+\mathrm{i}\gamma)\,\tilde{v}_{lN} = \frac{\partial L_l(\alpha,\beta,\omega)}{\partial(\mathrm{i}\omega)}\frac{\partial \tilde{v}_{l,N-1}}{\partial t} + \frac{\partial L_l(\alpha,\beta,\omega)}{\partial(\mathrm{i}\omega)}v_{l0}F_{lN} + Q_{lN}\,\mathrm{e}^{\gamma_l t}. \tag{2.14}$$

In order to prevent the secular growth of v_{lN} with respect to the 'fast' variables (x, z, t), the solvability condition (orthogonality to the solution of the adjoint OS-equation v_l^+) has to be satisfied. This defines F_{lN} as

$$F_{lN} = \left\langle \frac{\partial L_l(\alpha,\beta,\omega)}{\partial(-\mathrm{i}\omega)}v_{l0}\right\rangle^{-1}\left\langle Q_{lN}\,\mathrm{e}^{\gamma_l t} + \frac{\partial L_l(\alpha,\beta,\omega)}{\partial(\mathrm{i}\omega)}\frac{\partial v_{l,N-1}}{\partial t}\right\rangle, \tag{2.15}$$

where $\langle f\rangle = \int_0^\infty v_l^+ f\,\mathrm{d}y$. Substitution of (2.15) in (2.7) leads to a system of l amplitude equations. As $v \neq 0$, the expressions for η_{lN} follow immediately from (2.12).

In the case $v \equiv 0$ (Squire-mode disturbance), $L^{(1)}$ plays the role of the basic operator, and the above procedure can be applied in the same manner with respect to η_{lN}.

First-order ($\sim \epsilon^1$) amplitude equations are as follows:

$$\left(\frac{\partial}{\partial t} + W_{1l}\frac{\partial}{\partial x} + W_{2l}\frac{\partial}{\partial z}\right)A_l = \gamma_l A_l + \epsilon\sum_{j,k} S_{ljk}\,h_{l,j+k}\,A_j\,A_k, \tag{2.16a}$$

where

$$(W_1, W_2)_l = \left\langle \frac{\partial L_l(\alpha,\beta,\omega)}{\partial(-\mathrm{i}\omega)}v_{l0}\right\rangle^{-1}\left(\left\langle \frac{\partial L_l(\alpha,\beta,\omega)}{\partial(\mathrm{i}\alpha)}v_{l0}\right\rangle, \left\langle \frac{\partial L_l(\alpha,\beta,\omega)}{\partial(\mathrm{i}\beta)}v_{l0}\right\rangle\right), \tag{2.16b}$$

and
$$S_{jlk} = \langle H(\{0\},\{0\},f_{j0},f_{k0})\rangle\left\langle \frac{\partial L_l(\alpha,\beta,\omega)}{\partial(-\mathrm{i}\omega)}v_{l0}\right\rangle^{-1} \tag{2.16c}$$

denote group velocity and nonlinear interaction coefficients, respectively. At this order,

the behaviour of harmonics ($s \neq l$) and of mean flow distortion ($s = 0$) is defined by the locally parallel approximation:

$$L_s(\alpha, \beta, \omega)\, v_{s1} = H_{lj}(A_l f_{l0})\, \delta(s, l+j), \tag{2.17a}$$

$$L_s^{(1)}(\alpha, \beta, \omega)\, \eta_{s1} = -\mathrm{i}U'\beta_s v_{s1} + H_{lj}^{(1)}(A_l f_{l0}, A_j f_{j0})\, \delta(s, l+j), \tag{2.17b}$$

$$\left(\frac{\partial}{\partial t} + U\frac{\partial}{\partial x} - \frac{1}{Re}\frac{\partial^2}{\partial y^2}\right)\frac{\partial^2 v_{01}}{\partial y^2} + U''\frac{\partial}{\partial x}v_{01} = \sum_l |A_l|^2 H_{-l,l}(f_{l0}, f_{l0}^*), \tag{2.18a}$$

$$\left(\frac{\partial}{\partial t} + U\frac{\partial}{\partial x} - \frac{1}{Re}\frac{\partial^2}{\partial y^2}\right)\eta_{01} + U'\frac{\partial}{\partial z}v_{01} = \sum_l |A_l|^2 H_{-l,l}^{(1)}(f_{10}, f_{10}^*), \tag{2.18b}$$

$$f_{-l} = f_l^*, \quad H_{ij}(\{n_i = 0\}, \{m_i = 0\}, f_{i0}, f_{j0}) = H_{ij}(f_i, f_j).$$

Second-order ($\sim \epsilon^2$) amplitude equations have the form

$$\left\{\frac{\partial}{\partial t} + W_{1l}\frac{\partial}{\partial x} + W_{1l}\frac{\partial}{\partial z} - \gamma_l - \frac{\mathrm{i}}{2}\left(\frac{\partial^2\omega_l}{\partial\alpha^2}\frac{\partial^2}{\partial x^2} + 2\frac{\partial^2\omega_l}{\partial\alpha\,\partial\beta}\frac{\partial^2}{\partial x\,\partial z} + \frac{\partial^2\omega_l}{\partial\beta^2}\frac{\partial^2}{\partial z^2}\right)\right\} A_l$$

$$= \epsilon\sum_{j,k}\left[\left\{S_{ljk}A_jA_k + \epsilon\left(C_{ljk}^{(1)}\frac{\partial A_j}{\partial x} + C_{ljk}^{(2)}\frac{\partial A_j}{\partial z}\right)A_k\right\}h_{l,j+k} + \epsilon\sum_r C_{ljkr}h_{l,j+k+r}A_jA_kA_r\right]. \tag{2.19}$$

Terms containing $(\partial^2 A/\partial x^2, \partial^2 A/\partial z^2, \partial^2 A/\partial x\,\partial z)$ appear due to the dispersion, and may be omitted as $\mu \ll \epsilon$.

The first-order equations (2.19) describe a three-wave resonant interaction which in the simplest case (if $S_{ljk}h_{l,j+k} \neq 0$) is realized in the isolated wave triad $(j,k,l) = 1, 2, 3$. The four-wave resonance, two- and three-wave non-resonant interaction and self-modulation are all accounted by the term C_{ljkr} of the next (ϵ^2) order. Terms $\sim C_{ljk}^{(1,2)}$ correct the effect of three-wave resonance, and appear only in the case of a spatial perturbation evolution.

Some simplifications of (2.19) can be made provided that the primary flow is stationary and uniform in the z-direction (circumstances which are realized as far as typical experiments with vibrating ribbons in boundary layers are concerned), dimensional frequency and spanwise wavenumbers are constant, $A_l(x_0, t, z) = A_l(x_0) =$ const, wave evolution occurs only in the downstream direction ($\partial A_l/\partial t = \partial A_l/\partial z = 0$), and the condition $\mu \ll \epsilon$ holds.

In the Blasius-type flows of concern, the non-parallelism changes linear growth rates noticeably but had little influence on the nonlinear interaction (see, for example, Itoh 1974; Gaster 1974; Saric & Nayfeh 1975; Zelman & Kakotkin 1982) and can not compete with resonant effects, the analysis of which is the purpose of the present work. Accounting for non-parallelism in wave evolution will be specially emphasized (§3.3).

Until now we have not specified any particular type of linear eigenmodes θ_l. In boundary-layer flow of Blasius-type, the only modes which are susceptible to effective weakly nonlinear amplification are TS waves in the vicinity and within the region of the neutral stability curve. The possibility of the Squire-mode participation in S-transition will be discussed in a later section.

3. Symmetrical triads

3.1. *The resonance mechanism*

As mentioned earlier, a possible model for the main structure of S-transition may be a symmetric resonant triad of TS-waves (figure 1*c*), a special case ($\theta_1 = \theta_2 + \theta_3$) of which was considered for the first time by Craik (1971). In this section we investigate

Re	S_{1r}	S_{1i}	S_r	S_i
523	0.2	−0.1	2.75	−0.03
640	0.23	−0.015	4.51	−0.9
756	0.3	0.4	8.2	−3.2

TABLE 1. Interaction coefficients for a symmetrical subharmonic triad. $F_1 = 115 \times 10^{-6}$, $\beta/Re = 0.22 \times 10^{-3}$.

the evolution of resonant triads and its connection with the S-transition mechanism in the context of controlled vibrating ribbon experiments.

We consider a triad of TS-waves with spectral parameters $(\omega_1, \alpha_1, \beta_1 = 0)$, $(\omega_2 = \omega, \alpha_2 = \alpha, \beta_2 = \beta)$, $(\omega_3 = \omega, \alpha_3 = \alpha, \beta_3 = -\beta)$, $\omega_1 = 2\omega = \text{const}$, $\alpha_1 - 2\alpha = \Delta\alpha$. Then (2.16*a*) for $A_l(x) = b_l(x)\exp(\mathrm{i}\psi_l)$, $b_l = |A_l|$, $l = 1, 2, 3$ become

$$\left(W_1 \frac{\mathrm{d}}{\mathrm{d}x} - \gamma_1\right) A_1 = S_1 h_1 A_2 A_3, \tag{3.1a}$$

$$\left(W \frac{\mathrm{d}}{\mathrm{d}x} - \gamma\right) A_{2,3} = Sh A_1 A^*_{3,2}, \tag{3.1b}$$

$$A_l(x_0) = b_{l0} \mathrm{e}^{\mathrm{i}\psi_{l0}}, \quad l = 1, 2, 3, \tag{3.1c}$$

where we have taken into account that

$$\left.\begin{aligned} &W_{12} = W_{13} = W, \quad \gamma_2 = \gamma_3 = \gamma, \quad S_{2,1-3} = S_{3,1-2} = S, \\ &W_{11} = W_1, \quad S_1 = S_{1,2+3}, \quad h(\Delta\alpha) = h_{2,1-3} = h_{3,1-2}, \\ &h_1(\Delta\alpha) = h(-\Delta\alpha) = h_{1,2+3}, \quad h = \frac{1}{X}\int^{x+X} \exp\left[i\int^x \Delta\alpha \,\mathrm{d}x\right]\mathrm{d}x \approx \frac{\mathrm{e}^{\mathrm{i}\Delta\alpha X} - 1}{\mathrm{i}\Delta\alpha X}. \end{aligned}\right\} \tag{3.2}$$

Coefficients of equations (3.1) and (3.2) are determined by locally parallel Orr–Sommerfeld eigensolutions. This leads to the dependence of the solution of (3.1), (3.2) not only on the initial values A_{l0} but on local quantities $(\Delta\alpha, \beta, Re)$ as well.

In the numerical calculations which are reported below, the following algorithm is used. For given Reynolds number Re, physical frequency and spanwise wavenumbers, the OS-problem (2.13) is solved for each wave component. The solution uses an orthonormalization scheme. A Newton–Raphson iteration scheme converges to the eigenvalues. Then the corresponding vorticity component equations are solved. After that the integrals appearing in the definitions of coefficients (2.16*b*, *c*) are numerically evaluated.

This procedure is repeated parametrically for a selected interval of Reynolds numbers (parameters β_j/Re and $F_j = \omega_j/Re$ are kept constant). Then amplitude equations (3.1) are solved using a fourth-order-accurate Runge–Kutta procedure.

In table 1 some typical values of coefficients S_1, S are shown as an example.

For typical values $\alpha \sim 10^{-1}$, $\epsilon \sim 10^{-3}$ we have from (2.10) the estimate $10 < X < 10^3$, and in the following calculations values $X = 130$ to 150 are used.

Figure 2 shows the typical behaviour of amplitude b_{l0} and phase $\Delta\psi = \psi_1 - \psi_2 - \psi_3$ for $b_{10} > b_{20} > b_{30}$. In the early stage, $Re \leqslant Re_n$, a parametric amplification of subharmonics takes place. Their amplitudes b_2, b_3 increase rapidly without changing the behaviour of the fundamental wave amplitude b_1, and spontaneously equalize their levels: $b_2 = b_3 = b$. When $b_{2,3} \geqslant b_1$ $(Re \geqslant Re_n)$ disturbances enter a nonlinear development region that involves an explosive amplification of all triad components along with phase localization, $\Delta\psi \to 0$. In the region of parametric amplification

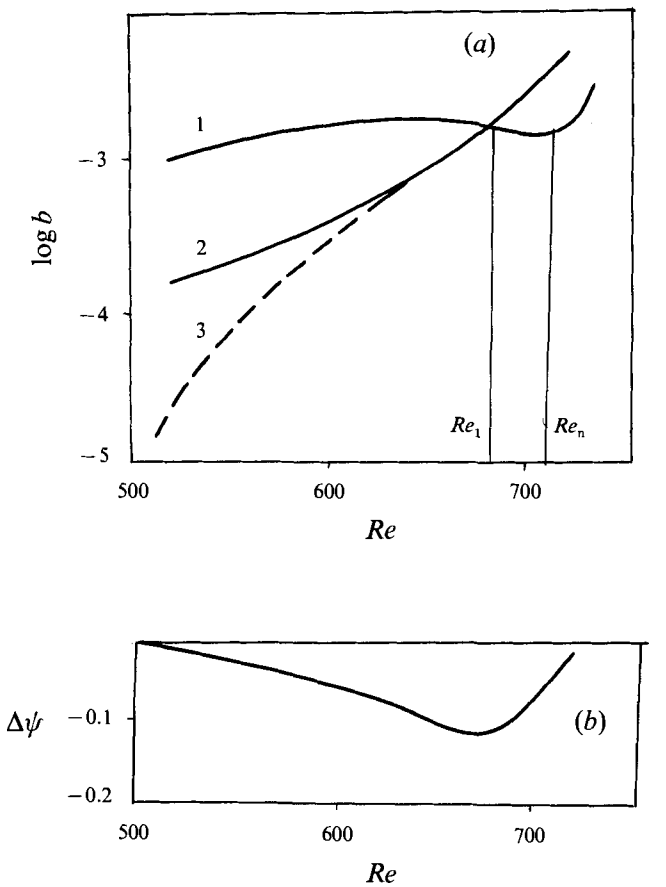

FIGURE 2. (*a*) Amplification curves for triad components: curve 1, two-dimensional fundamental; curves 2, 3, symmetrical subharmonics; (*b*) Phase localization. $F_1 = 115 \times 10^{-6}$; $\beta/Re = 0.18 \times 10^{-3}$.

($|A_1| \gg |A_{2,3}|$) the following conditions come from the ratio of linear and nonlinear terms:

$$|\gamma_1| > \left|\frac{A_2 A_3}{A_1} S_1 h_1\right|, \quad |\gamma| < |A_1 Sh|. \tag{3.3}$$

The first condition ensures an independent two-dimensional wave evolution, and the second the predominance of the parametric growth rate over the linear one. Coefficients ratios $|S/S_1| \sim 10$ (see table 1), $\gamma_1 \sim \gamma$, which are valid in boundary layers, keep the above conditions valid not only when $|A_1| \gg |A_{2,3}|$, but when $|A_{2,3}| \approx |A_1|$ as well ($|\gamma_1| > |S_1 A|, |\gamma| < |SA_1|$). This fact ensures the applicability of linear parametric analysis (the secondary instability method of Nayfeh 1987; Herbert 1988; Fischer & Dallmann 1991, for example) in the régime where it formally fails. We emphasize that this circumstance may be clarified only by a nonlinear analysis.

The process of parametric amplification displays a threshold character. A threshold value b_{1*}, above which (i.e. for which $b_1 > b_{1*}$) parametric resonance is effective, follows from (3.3) as $b_{1*} = |\gamma/Sh|$. A solution of (3.1) in the region of parametric evolution can be expressed in analytic form and points to the double-exponential growth of subharmonic amplitudes:

$$A = Z_\nu(\tilde{z}) \exp\left[\left(\frac{2\gamma}{W} + \frac{\gamma_1}{W_1}\right) x\right], \tag{3.4}$$

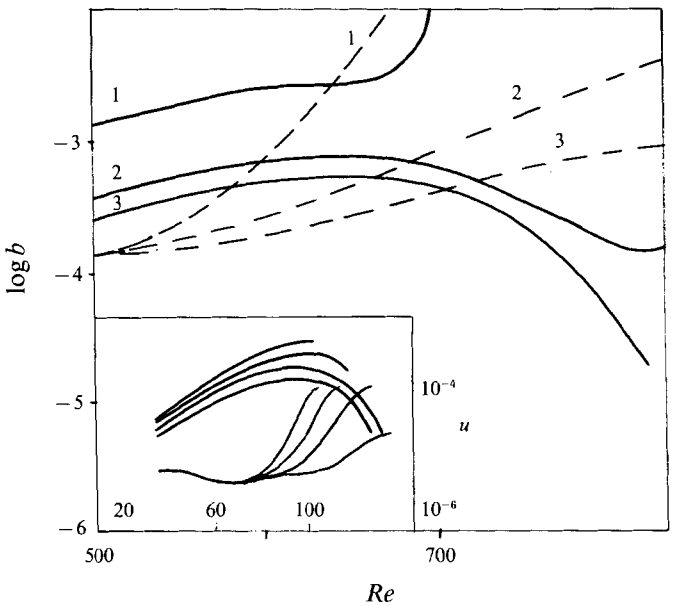

FIGURE 3. Amplification curves for various two-dimensional fundamental amplitudes: solid lines, fundamental; dashed lines, subharmonics. $F_1 = 115 \times 10^{-6}$; $\beta/Re = 0.18 \times 10^{-3}$. For comparison the inset shows experimental data by Gaster (1984) for downstream r.m.s. velocity.

where

$$\nu = \tfrac{1}{2}, \quad \tilde{z} = (\mathrm{i}|Sh|\, b_{10}\, W_1/\gamma_1)\exp(\gamma_1 x/W_1), \quad z_{\frac{1}{2}}(\tilde{z}) = (2/\pi\tilde{z})^{\frac{1}{2}}(C_1 \sin\tilde{z} + \tilde{C}_2 \cos\tilde{z})$$

is a Bessel function, and

$$\sigma = \frac{\mathrm{d}A}{A\,\mathrm{d}x} \approx \left\{\left(\frac{2\gamma}{W} + \frac{\gamma_1}{2W_1}\right) + \left|\frac{Sh W_1 A_{10}}{\gamma_1}\right| \exp\frac{\gamma_1 x}{W_1}\right\}. \tag{3.5}$$

Exponential growth of the amplification rates for $b_{2,3}$ is clearly seen from figure 2. Amplification curves for different b_1 are shown in figure 3, from which the crucial role of the two-dimensional wave amplitude can be seen. An initial phase variation $\Delta\psi(x_0)$ changes the behaviour of $b_{2,3}$ at early stages, but does not influence the amplification law as a whole (figure 4). The main effect of variation of the initial values $\Delta\psi_0, b_{20}, b_{30}$ (figure 5) is a shift of the 'nonlinear point' Re_n in relation to the neutral curve for two-dimensional waves. Thus an equalization $b_1(Re_i) = b(Re_i)$ inside the neutral curve ($Re_i \leqslant Re, \gamma_1(Re) > 0$) leads immediately to the growth of all triad components (curve 1, figure 3): $Re_n \approx Re_i$; whereas outside the neutral curve ($\gamma_1(Re) < 0$) an amplification of subharmonics does not prevent the damping of b_1 (curve 2, figure 3) to some level. At that level Re_n shifts downstream and $(Re_n - Re_i)$ increases. Further shift of Re_i towards the stable region may destroy completely the nonlinear interaction ($Re_n \to \infty$) (curve 3, figure 3). Nevertheless, in all cases the resonant interaction in symmetrical TS-triads demonstrates the existence of a mechanism leading to rapid growth of perturbations with half the fundamental frequency, and to the spontaneous symmetrization of the three-dimensional oscillation field, which are the properties inherent in S-transition (Kachanov & Levchenko 1982, 1984; Corke & Mangano 1989).

3.2. *Preferred wave angles*

The mechanism described above has been established as effective for a wide range of wave vectors $\boldsymbol{k}_{2,3}$ of the oblique waves comprising a resonant triad. The occurrence of

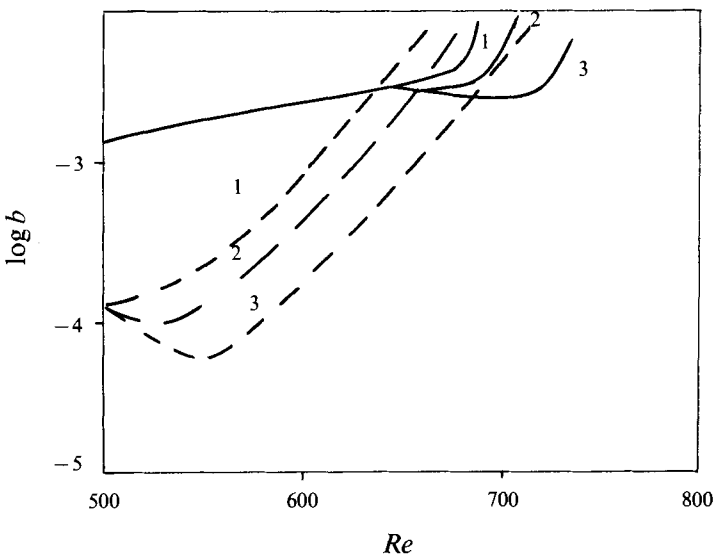

FIGURE 4. Amplification curves for various initial phases $\Delta\psi_0$: curve 1, 0; curve 2, $\frac{1}{2}\pi$; curve 3, π. $F_1 = 115 \times 10^{-6}$; $\beta/Re = 0.18 \times 10^{-3}$.

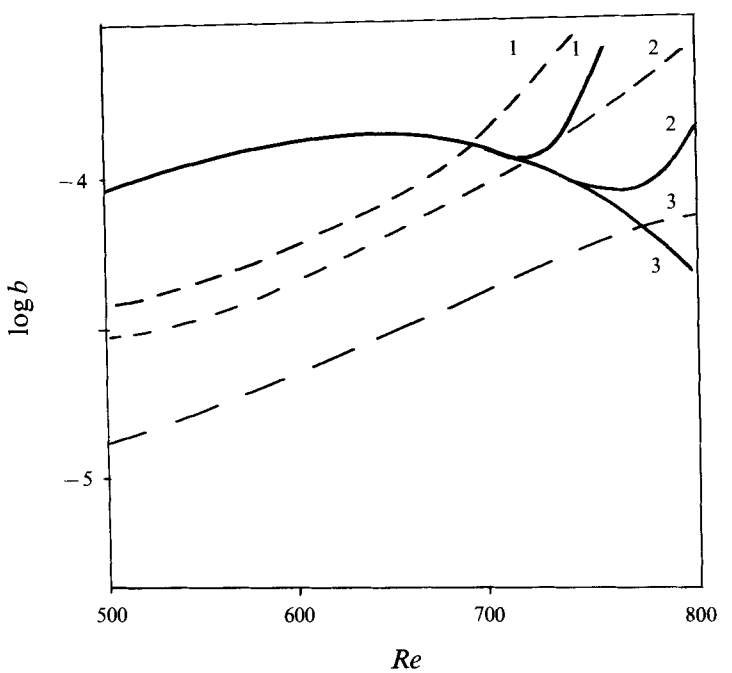

FIGURE 5. Amplification curves for various subharmonic initial amplitudes: solid lines, two-dimensional fundamental; dashed lines, subharmonics. $F_1 = 115 \times 10^{-6}$; $\beta/Re = 0.18 \times 10^{-3}$.

S-transition spatial structure arising from a homogeneous spectrum of background disturbances, poses the problem of preferential wave angles. To study this problem the relationship between subharmonic amplification rate and wave angle $\lambda = |\beta/\alpha|$ was considered. Parametric growth rate is related to λ through the coefficients of amplitude equations (3.1). Figure 6(*a*) shows the variation of $|Sb_{10}|$ and $|h|$ with λ. It is easy to see

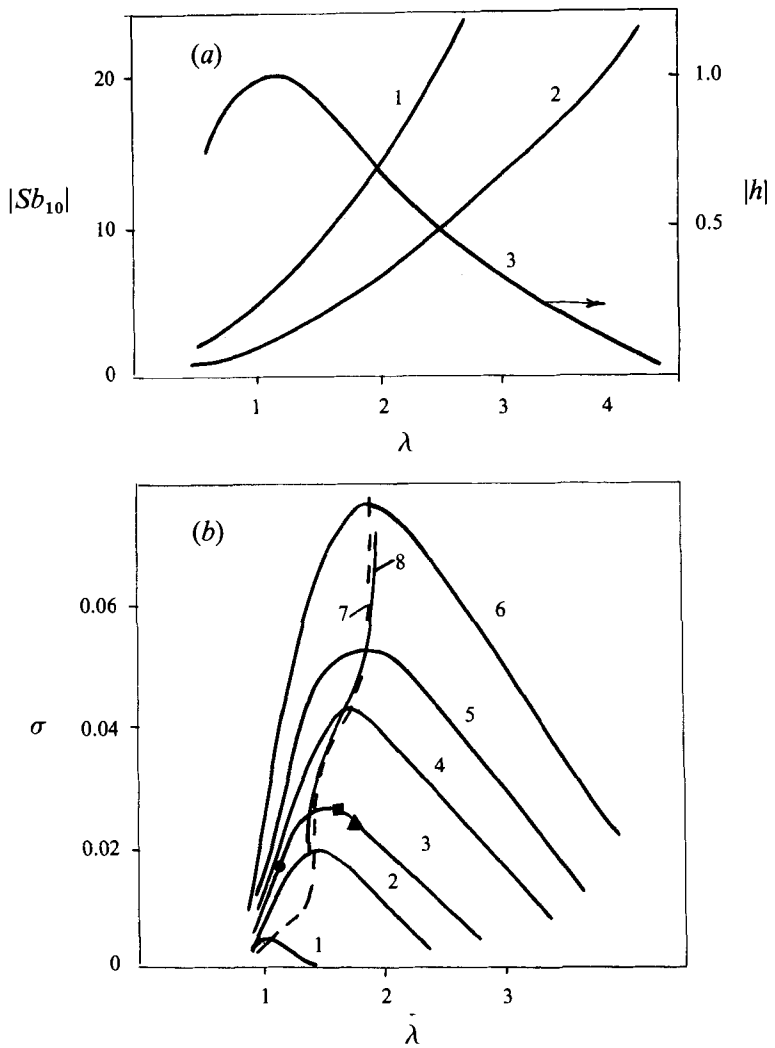

FIGURE 6. (*a*) Variation of $|Sb_{10}|$ (curves 1, 2) and $|h|$ (curve 3) with λ: curve 1, $b_{10} = 10^{-3}$; 2, $b_{10} = 2\times10^{-3}$. $F_1 = 115\times10^{-6}$, $Re = 640$, $X = 130$. (*b*) Local growth rate versus λ for various two-dimensional wave amplitudes: curve 1, $b_1(Re_{II}) = 0.0014$; 2, 0.0021; 3, 0.0028; 4, 0.0032; 5, 0.004; 6, 0.0053; $F_1 = 115\times10^{-6}$; $Re = 640$. Preferred λ_m for ($F_1 = 115\times10^{-6}$, $Re = 640$) (curve 7) and ($F_1 = 75\times10^{-6}$, $Re = 890$) (curve 8). Experimental points are from Corke & Mangano (1989).

that $|Sb_{10}|$ and $|h|$ are growing, and Gaussian-like functions of λ, respectively. As a result the parametric growth rate $\sigma(\lambda, b_{10})$ reaches the maximum value σ_m for certain a λ_m depending on the initial amplitude of the two-dimensional TS wave. Figure 6(*b*) shows the growth rate $\sigma(\lambda)$ for various amplitude levels b_{10}. For $b_{10} \approx b_{1*}$ (weak supercriticality), $\lambda_m \approx 1$ which corresponds to Craik's triad with $\theta_1 = \theta_2 + \theta_3$ (curve 1, figure 6*b*). Once the amplitude of the two-dimensional wave increases, the region where $\sigma > 0$ grows, and σ_m shifts towards a higher value of λ (curves 2–6, figure 6*b*) (where $\Delta\alpha \neq 0$) and reaches an asymptote at $\lambda_m \approx 2$. Calculations showed that the function $\lambda_m = \lambda_m(b_{10})$ is invariant with respect to ω and Re (curve 7, figure 6*b*). This implies that the selected disturbance with the maximum growth maintains the propagation angle defined by the same function $\lambda_m(b_{10})$ throughout the downstream evolution (curve 5, figure 7). In the case of a homogeneous background, a selection of oscillations with

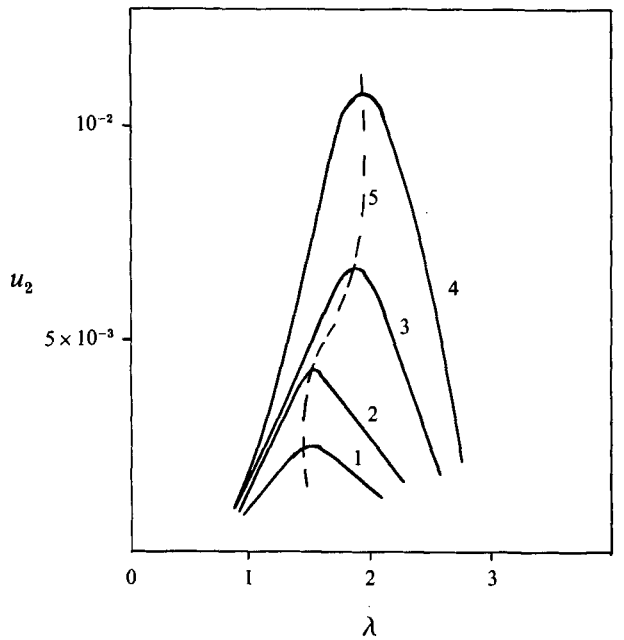

FIGURE 7. Subharmonic intensities u_2 for various b_1 (Re_{II}): curve 1, 0.25%; 2, 0.35%; 3, 0.43%; 4, 0.5%. Preferred λ_m (curve 5). $F_1 = 115\times10^{-6}$, $Re = 640$.

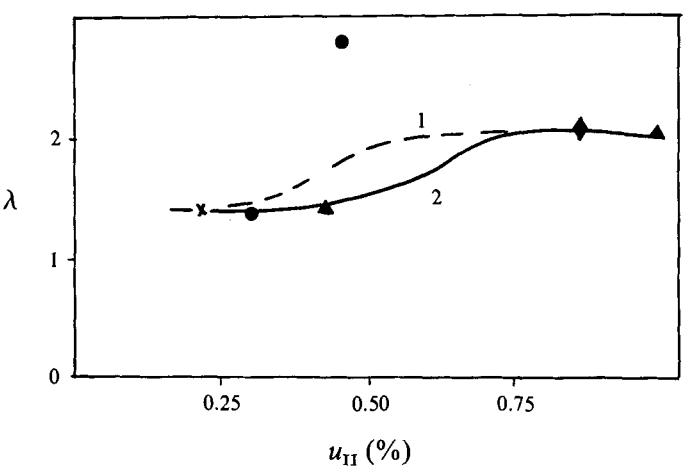

FIGURE 8. The value of λ for the most amplified subharmonics as a function of r.m.s. intensity of the two-dimensional fundamental (curve). Curve 2, the same but with non-parallelism. Experimental data: ▲, Saric *et al.* (1984); ●, Saric & Thomas (1984); ×, ◆, Kachanov & Levchenko (1984).

respect to their amplification rates provides a selection of waves whose amplitudes dominate with the corresponding directions of propagation. The angular distribution of the disturbance field is determined by the initial amplitudes of the two-dimensional wave.

3.3. *Comparison with experiments and computations*

The results obtained completely explain the process of formation and further development of the S-transition dominant structures seen in experiments. Figure 8 shows the function $\lambda_m(u_{II})$ (curve 1), where u_{II} repreents the two-dimensional wave velocity on the upper branch of the stability diagram. Accounting for non-parallelism

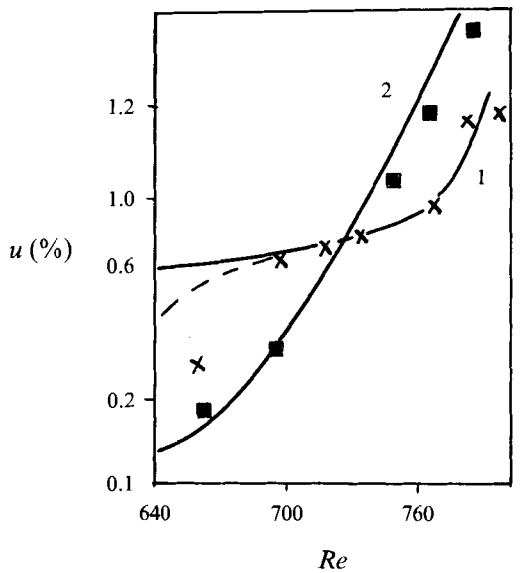

FIGURE 9. Disturbance intensity growth: curve 1, two-dimensional; 2, subharmonics. Dashed curve includes non-parallelism in linear growth rate. Experimental data by Saric *et al.* (1984). $F_1 = 106 \times 10^{-6}$, $\beta/Re = 0.2 \times 10^{-3}$.

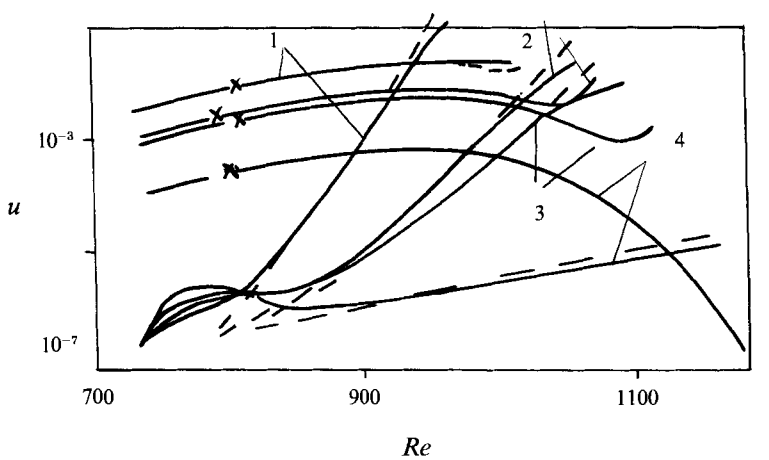

FIGURE 10. Amplification curves for different two-dimensional wave intensities (curves 1–4). Dashed curves represent the present investigation, solid curves the numerical experiment by Spalart & Yang (1987). Symbols × mark a two-dimensional wave. $F_1 = 76 \times 10^{-6}$.

(Zelman & Kakotkin 1982) shifts the middle part of curve 1 and produces excellent agreement between the theory (curve 2) and observations. Numerically obtained growth rates versus wave angles (curve 3, figure 6) practically coincide with experimental data by Corke & Mangano (1989). Amplification curves for triad components (figure 9) demonstrate good agreement with the observations by Saric *et al.* (1984). The different behaviour of the amplitudes ('dog's leg') in the early stages of interaction ($Re < 700$) can be explained by the imperfection of experiments (Thomas 1983; Saric *et al.* 1984). At the stage, $Re > Re_n$, of essentially nonlinear development ($(b, b_1) > 10^{-2}$) higher-order nonlinear effects come into play.

Our numerical results (figure 10), based on (3.1), are consistent with the data from computational simulations of the Navier–Stokes equations (Spalart & Yang 1987) and

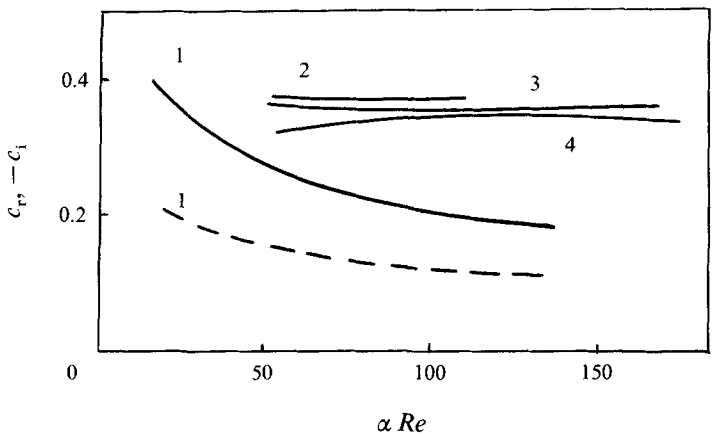

FIGURE 11. Phase velocities (solid curves, real part; dashed curve, imaginary part): curve 1, Squire mode, $F = 62 \times 10^{-6}$; curves, 2, 3, 4, two-dimensional TS-mode, $F_1 = (145, 115, 68) \times 10^{-6}$.

with those (curve 8, figure 6) obtained by the secondary instability method (Herbert 1984). All this supports the capability of the elementary model including TS-triads to provide a satisfactory explanation and a quantitative characterization of the S-transition dominant structure.

3.4. *TS and Squire modes in Blasius flow*

As mentioned in the Introduction, the problem of the nature of subharmonic waves in S-transition in Blasius flow is still of principle significance. This problem originated from speculation about two different (C and H) mechanisms (Saric & Thomas 1984; Herbert 1988) which could be responsible for the dominant structure of the S-transition. The C-mechanism was attributed to the evolution of the perfectly synchronized ($\Delta\alpha = 0$) TS-triad, and was expected to operate at low amplitudes of the two-dimensional wave. The H-mechanism was expected to operate over a wide range of two-dimensional wave amplitudes, and to originate from the selection of Squire modes (Herbert 1983, 1984).

To clarify the role of Squire vortices in S-transition we have analysed the solution of the homogeneous equation (2.2). Figure 11 displays the real and imaginary parts of the phase velocity c, which is invariant with respect to β with an accuracy of $O(Re^{-1})$. It can be seen from this figure that Squire modes are highly damped over the whole range of Re where two-dimensional TS-modes are unstable ($|\gamma_s| \sim \omega_s, \gamma_s < 0$). At that condition, the fundamental TS-wave and Squire subharmonics are far from resonance:

$$|\omega_{\mathrm{TS}}(2\alpha) - 2\omega_{\mathrm{Sq}}(\alpha)| \sim |\gamma_s(\alpha)| \sim |\omega_s|.$$

It should be noted that according to our numerical results the TS-wave velocities are significantly higher than those for Squire modes: $\max|v_2^{\mathrm{Sq}}/v_2^{\mathrm{TS}}| \leqslant 0.1$ provided that the initial intensities of vortices, $\max|\eta_0(y)|$, are equal. That makes an excitation of Squire modes all the more difficult. Moreover, the local streamwise velocity y-profile of the Squire subharmonic is quite different from that for TS-modes, which is entirely consistent with the observations (figure 12). The properties noted indicate the lack of effective weakly nonlinear interaction between TS-fundamental and Squire subharmonics in Blasius flow and prevents the amplification of Squire modes at the low amplitudes of interest. Therefore, the participation of Squire modes in S-transition on a flat plate is hardly probable. At the same time, the analysis of TS-triad evolution

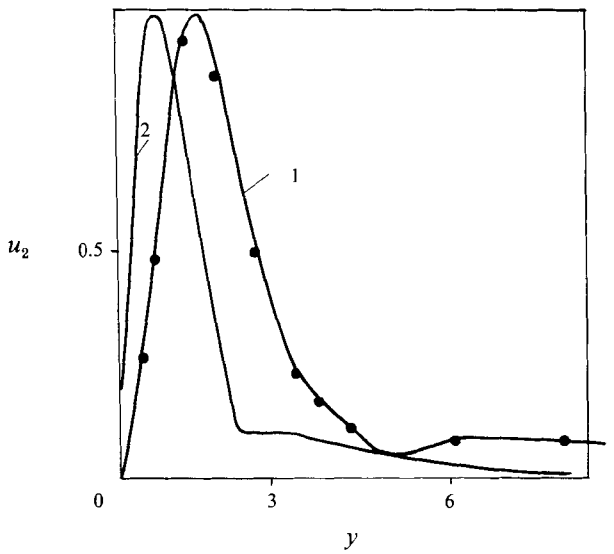

FIGURE 12. Normalized local velocity profiles for TS (curve 1) and Squire (curve 2) subharmonics. Experimental data by Kachanov & Levchenko (1984).

provides an adequate explanation of the S-transition process. (Note that the nature of the waves which provide the dominant structure of S-transition may be experimentally tested by pressure gradient measurements across the boundary layer. This value in the Squire modes is constant, quite unlike the TS-modes.) The H-mechanism concept originated primarily from the investigation of Poiseuille flow (Herbert 1983), where resonance in TS-triads with symmetrical OS-eigenfunctions is inoperative. But the speculation noted is doubtful even in Poiseuille flow, because the occurrence of resonant TS-triads may be explained on the basis of non-symmetrical OS-solutions (with respect to the channel axis) (Goldshtik, Lifshits & Stern 1984; Zhao & Zhao 1988).

We conclude that the suggested mechanism for formation of the S-transition dominant structure in Blasius boundary layer has a universal character, and it is connected with the selection and symmetrization of background three-dimensional TS-disturbances which propagate in the direction determined by the primary TS-wave. As a result, the dominant symmetrical TS-triad is formed (with the C-triad as a special case at low two-dimensional wave amplitudes).

3.5. *Streamwise pressure gradient*

The features of S-transition in boundary layers with a streamwise pressure gradient is of practical interest. The problem was treated in Herbert & Bertolotti (1985) by the secondary instability method. We considered (Zelman & Maslennikova 1989) pressure gradient effects on the formation and evolution of symmetrical TS-triads with Falkner–Skan profiles as a model problem. In this case $U_\infty(x) \sim x^{m_1}$ and the local pressure gradient $\nabla p = \partial p/\partial x \sim m$, where $m = 2m_1/(m_1+1)$.

The system of amplitude equations and procedure for obtaining coefficients does not differ from the case of Blasius flow, (3.1) and (3.2).

Numerical results showed that the pressure gradient $\nabla p \neq 0$ did not change the general picture of the evolution of resonant TS-triads. Coefficients S_{ijk} changed weakly, so the variation of subharmonic amplification rates was defined by changes in the two-dimensional wave linear growth rates. Figure 13 presents a comparison of triad

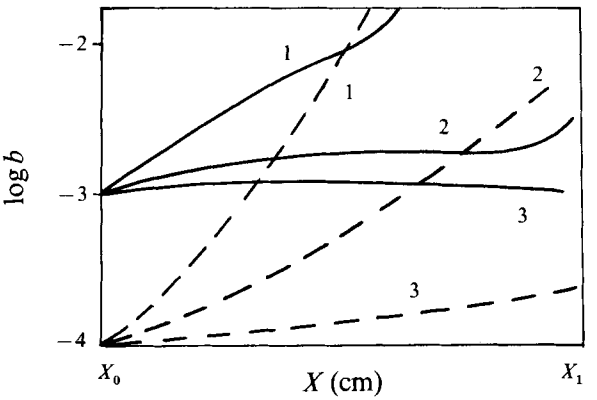

FIGURE 13. Amplification curves for Falkner–Skan profiles (solid curves, fundamental; dashed curves, subharmonics) for $m = -0.1$ (curve 1), $m = 0$ (2), $m = 0.1$ (3). $F_1 = 115 \times 10^{-6}$.

evolution, for $m = -0.1, 0, +0.1$, along a fixed dimensional interval (x_0, x_1). Growth rates of all triad components increased when the pressure gradient changed from positive ($m > 0$) to negative ($m < 0$). The three-dimensional wave selection mechanism which was responsible for the dominant structure operated at the parametric stage, and was associated with the dependence of $(h_{l,j+k}, S_{ljk})$ on λ just in Blasius flow. In the case $m > 0$ (as well as $m = 0$) the function $\lambda_m(b_{10})$ turned out to be constant with respect to Re, in contrast with the case $m < 0$ where $\lambda_m(b_{10})$ increased with increasing Re, and for different b_{10} varied in the range $1.2 < \lambda_m < 3$. Such behaviour caused a spatial spectrum broadening of the background disturbances excited in the evolution process. Along with increased linear growth rates, the spectrum broadening served as an extra destabilizing factor. The second special feature of flows with $m < 0$ was a reduction in the size of the nonlinear interaction region: explosive growth of triad components began immediately at the location $Re_i = Re_n$ where all amplitudes became equal.

4. Non-symmetrical and multiwave interactions

4.1. *Interaction in a five-wave system*

Although the symmetric subharmonic triad considered in the preceding section enables us to model the basic structure of S-transition, it is a very simplified model. Since there is a broad spectrum of disturbances which can interact resonantly with the primary two-dimensional wave, the problem for their mutual interaction arises. The simplest model accounting for this effect is a five-wave system comprising a two-dimensional wave $(A_1, 2\omega_1, \alpha_1, \beta_1 = 0)$ and two pairs of three-dimensional waves $(A_{2,3}, \omega_{2,3} = \omega, \alpha_2 = \alpha_3, \beta_2 = -\beta_3)$, $(A_{4,5}, \omega_{4,5} = \omega, \alpha_4 = \alpha_5, \beta_4 = -\beta_5)$. Close to the resonances $(h_{i,j+k} \approx \exp \mathrm{i}(\theta_j + \theta_k - \theta_i)$, $(i,j,k) = 1, \ldots, 5)$ equations (2.16*a*) take the form

$$\left(W_{11}\frac{\mathrm{d}}{\mathrm{d}x} - \gamma_1\right) A_1 = S_{1,2+3} B_2 B_3 + S_{1,4+5} B_4 B_5 + S_{1,4+3}(B_4 B_3 + B_5 B_2), \qquad (4.1a)$$

$$\left(W_{12}\frac{\mathrm{d}}{\mathrm{d}x} - \gamma_2\right) B_{2,3} + \frac{\mathrm{i}}{2}(W_{12}\Delta\alpha_1) \pm W_{22}\Delta\beta) B_{2,3} = A_1(S_{2,1-3} B^*_{3,2} + S_{2,1-5} B^*_{5,4}), \qquad (4.1b)$$

$$\left(W_{14}\frac{\mathrm{d}}{\mathrm{d}x} - \gamma_4\right) B_{4,5} + \frac{\mathrm{i}}{2}(W_{14}\Delta\alpha_2 \pm W_{24}\Delta\beta) B_{4,5} = A_1(S_{4,1-3} B^*_{3,2} + S_{4,1-5} B^*_{5,4}), \qquad (4.1c)$$

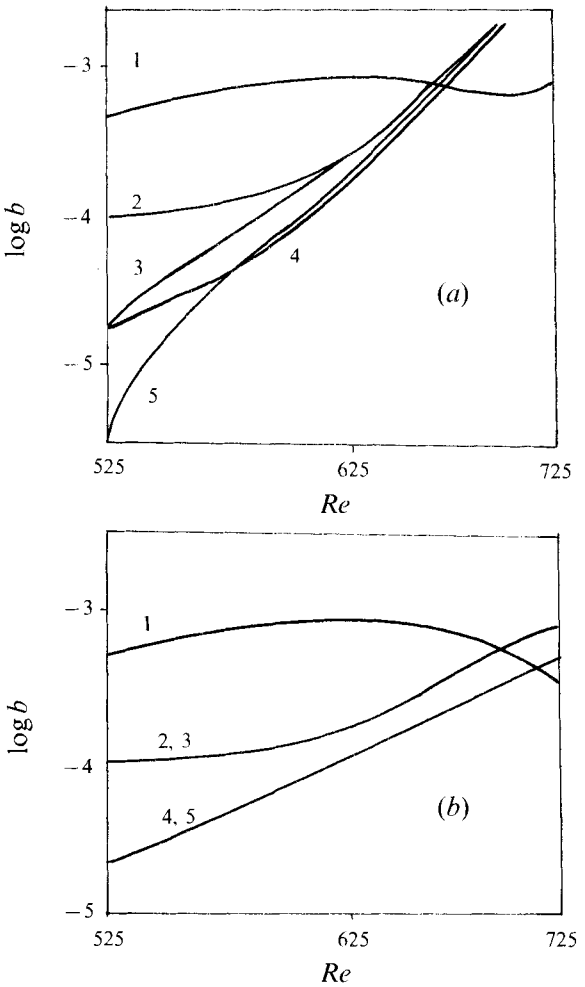

FIGURE 14. Amplification curves for five-wave system, (*a*) with and (*b*) without cross-interactions. $F_1 = 115 \times 10^{-6}$, $\beta_2/Re = 0.171 \times 10^{-3}$, $\beta_4/Re = 0.15 \times 10^{-3}$.

where

$$\Delta\alpha_{1,2} = \alpha_1 - (\alpha_{2,4} + \alpha_{3,5}), \quad \Delta\beta = |\beta_2 - \beta_4|, \quad B_{2,3} = A_{2,3} \exp\left[\tfrac{1}{2}\mathrm{i}\left(\int \Delta\alpha_1 \, \mathrm{d}x + \Delta\beta z\right)\right],$$

$$B_{4,5} = A_{4,5} \exp \tfrac{1}{2}\mathrm{i}\left(\int \Delta\alpha \, \mathrm{d}x - \Delta\beta z\right).$$

Figure 14(*a*) shows an example of the amplitude evolution of such a five-wave system. Along with interactions in symmetrical triads, interactions in non-symmetrical triads occur, and are accounted for by the terms which contain $S_{1,4+3}$, $S_{2,1-5}$, $S_{4,1-3}$. A rapid growth of three-dimensional waves and equalization of their amplitudes originate from non-symmetrical interactions as was found by Maslennikova & Zelman (1985), and Zelman & Maslennikova (1985). The rate of spectrum excitation was found to be much less in the absence of such interactions (see figure 14*b*). It may be concluded that low-frequency spectrum broadening, clearly observed in S-transition (Corke & Mangano 1989), occurred not only because of the evolution of wave packets comprising

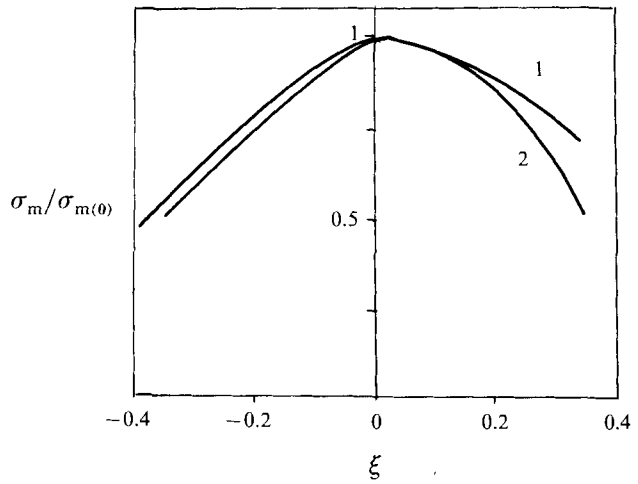

FIGURE 15. Normalized maximum parametrical growth rates for detuned subharmonics versus detuning parameter ξ at different $b_1(Re_{II})$: 0.0022 (curve 1), 0.0017 (curve 2).

independent symmetrical wave pairs, but also as a result of cross-exchange between them. Spatial localization of disturbances obtained in our calculations is supported by more general analysis of wave packet evolution (Gaster 1984; Zelman & Smorodsky 1988).

4.2. *Interaction in detuned triads*

In connection with the results presented above, the analysis of interaction in a triad of arbitrary type is of substantial interest.

We restrict our attention to analysis of the evolution of frequency-locked waves ($j = 1, 2, 3$), $\omega_1 = \omega_2 + \omega_3$ with arbitrary wave vectors. Equations (2.16*a*) take the form

$$\left.\begin{aligned}
\left(W_{11}\frac{\mathrm{d}}{\mathrm{d}x}-\gamma_1\right)A_1 &= S_{1,2+3}B_2B_3,\\
\left(W_{12}\frac{\mathrm{d}}{\mathrm{d}x}-\gamma_2\right)B_2+\frac{\mathrm{i}}{2}(W_{12}\Delta\alpha+W_{22}\Delta\beta)B_2 &= S_{2,1-3}AB_3^*,\\
\left(W_{13}\frac{\mathrm{d}}{\mathrm{d}x}-\gamma_3\right)B_3+\frac{\mathrm{i}}{2}(W_{13}\Delta\alpha+W_{23}\Delta\beta)B_3 &= S_{3,1-2}AB_2^*,\\
\Delta\alpha = \alpha_1-\alpha_2-\alpha_3,\quad \Delta\beta &= \beta_1-\beta_2-\beta_3,\\
B_{2,3} &= A_{2,3}\exp[\tfrac{1}{2}\mathrm{i}(\Delta\alpha x+\Delta\beta z)].
\end{aligned}\right\} \tag{4.2}$$

We considered in Zelman & Maslennikova (1992) the effects of low-frequency three-dimensional disturbance excitation in the field of a two-dimensional wave with $\boldsymbol{k}_1 = (\alpha_1, \beta_1 = 0)$. For this purpose a parametric growth rate

$$b_{2,3}^{-1}\frac{\mathrm{d}b_{2,3}}{\mathrm{d}x} = \sigma_{2,3}(b_{10}, \beta_2, \beta_3, \omega_2, \omega_3 = \omega_1-\omega_2)$$

was analysed. Figure 15 shows $\tilde{\sigma}(\pm\xi) = \max_{\beta_2,\beta_3}\sigma_{2,3}$ versus the detuning parameter $\xi = 1-2\omega_2/\omega_1$ for various b_{10}. It can be seen that $\tilde{\sigma}$ has a maximum at $\xi = 0$, which corresponds to the symmetrical triads investigated in §3. This proves their dominant role in the structure of S-transition. At the same time, the curves in figure 15 show the

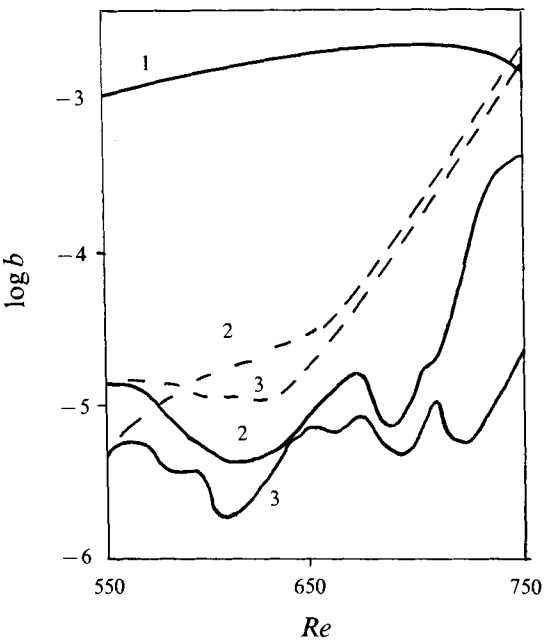

FIGURE 16. Amplification curves for detuned triad components at $\Delta\psi_0 = 0$ (dashed curves 2, 3) and $\Delta\psi_0 = \frac{3}{2}\pi$ (solid curves 2, 3). $F_1 = 105 \times 10^{-6}$, $F_2 = 38 \times 10^{-6}$, $F_3 = 67 \times 10^{-6}$, $\beta_2/Re = 0.168 \times 10^{-3}$, $\beta_3/Re = 0.263 \times 10^{-3}$. Solid curve 1: two-dimensional fundamental.

possibility of broadband spectrum excitation near half of the primary wave frequency. Such spectrum broadening is a typical feature of S-transition (Corke & Mangano 1989; Kachanov *et al.* 1984). Triad investigation in the general case $\beta_j \neq 0$ shows a rapid increase of low-frequency large-scale waves in the parametric region and supports the dominant role of symmetrical subharmonic triads in the transition process. However, some specific features were established. Subharmonic amplification rates were reduced, and in some cases the explosive growth in the nonlinear region was not realized. The evolution picture became more sensitive to the conditions of disturbance excitation, as can be seen from figure 16, where the behaviour of $b_j(Re)$ is shown for various initial phases $\Delta\psi_0$. It may be speculated that the sensitivity noted can promote the stochastization of the transitional flow field.

An interaction in non-symmetrical triads causes not only a spectrum broadening, but may be responsible for the formation of the dominant structure. Suitable conditions arise in inhomogeneous initial distributions of disturbances, as, for example, when three-dimensional waves are artificially induced in the flow. Such situation was probably realized in the experiment of Saric & Reynolds (1980). An excitation of oscillations with frequencies F_1 and F_4 led to anomalous growth of frequencies F_2 and F_3. Maslennikova & Zelman (1985) and Zelman & Maslennikova (1985) suggested that these observations could be explained by the formation and the evolution of detuned triads comprising two-dimensional wave F_1 and a pair of three-dimensional waves $F_{2,3}$ ($F_1 = F_2 + F_3$). A good correlation between experimental data and calculated disturbance velocities seems to support our speculation (figure 17).

The process of detuned mode generation in the experiments of Corke & Mangano (1989), where a two-dimensional wave with frequency F_1 and a symmetrical pair ($\alpha_2 = \alpha_3$, $\beta_2 = -\beta_3$, $F_2 = F_3 = \frac{1}{2}F_1 - \Delta F$) have been initially introduced into the flow, may be explained in the same manner. We suggest that the primary waves interact with

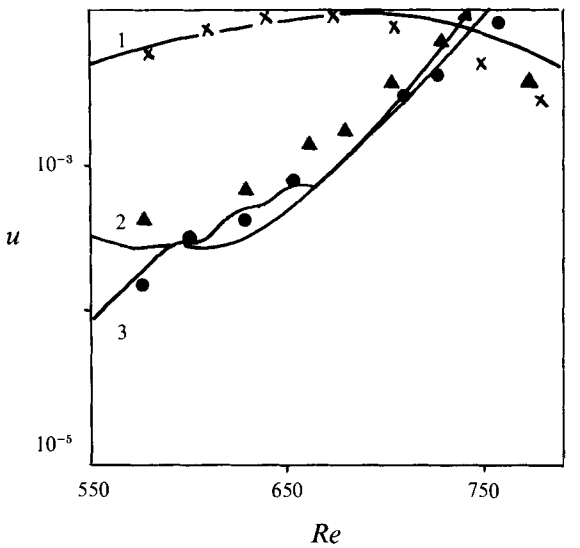

FIGURE 17. Disturbance velocity growth for detuned triad ($F_1 = 105 \times 10^{-6}$, $F_2 = 38 \times 10^{-6}$, $F_3 = 67 \times 10^{-6}$, $\beta_2/Re = 0.168 \times 10^{-3}$, $\beta_3/Re = 0.263 \times 10^{-3}$) in comparison with the experiment by Saric & Reynolds (1984).

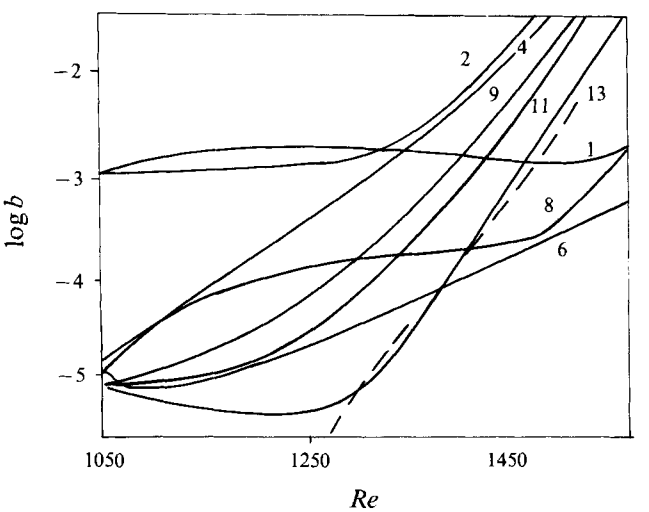

FIGURE 18. Amplification curves for multiwave detuned system: the numbers on the curves correspond to the j of F_j. $F_1 = 88 \times 10^{-6}$, $F_{2,3} = 39.5 \times 10^{-6}$, $F_{4,5} = F_1 - F_{2,3} = 48.5 \times 10^{-6}$, $F_{6,7} = \frac{1}{2}F_1 = 44 \times 10^{-6}$, $F_8 = 2F_{2,3} = 79 \times 10^{-6}$, $F_{9,10} = F_8 - F_{4,5} = 30.5 \times 10^{-6}$, $F_{11,12} = F_1 - F_{9,10} = 57.5 \times 10^{-6}$, $F_{13,14} = F_8 - F_{11,12} = 20.5 \times 10^{-6}$. Dashed curve shows three-dimensional wave $F_0 = F_1$.

background disturbances and form resonant triads of symmetrical and non-symmetrical types. Interaction between F_1 and $F_{2,3}$ leads to the growth of three-dimensional ($F_{4,5} = F_1 - F_{2,3}$, $F_{6,7} = \frac{1}{2}F_1$) and two-dimensional ($F_8 = 2F_2$) background disturbances. At the next step, a resonance between F_8 and $F_{4,5}$ leads to the growth of three-dimensional waves with $F_{9,10}$, and so on. Simultaneously two-wave non-resonant interaction occurs, which causes particularly intense amplification of a three-dimensional mode ($\sim A_{2,3}^2$) of fundamental frequency $F_0 = F_1$. Numerical results for

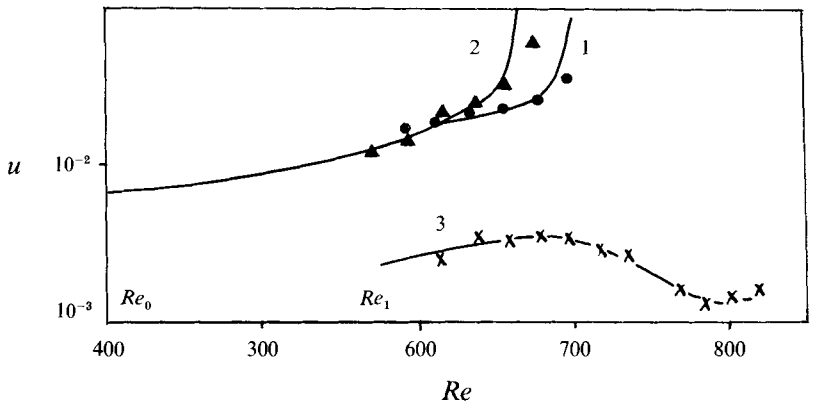

FIGURE 19. Active control of transition. Disturbance intensity behaviour in comparison with Thomas (1983) (symbols). Curve 1, the first vibrator only; curve 2, the second vibrator only; curve 3, two vibrators with $b_1(x_1) = \tilde{b}_1(x_1)$, $\phi(x_1) - \tilde{\phi}(x_1) = 0.96\pi$. $F_1 = 110 \times 10^{-6}$.

amplitude evolution based on the first-order equations (2.16*a*) are shown in figure 18. The detailed comparison in Zelman & Maslennikova (1992) reveals good agreement between the theoretical and experimental data.

Our results demonstrate the essential role of resonant interactions in detuned transition (transition due to detuned wave interaction), primarily as a mechanism for energy cascade to three-dimensional low-frequency large-scale disturbances. The effects of disturbance growth stabilization have not been achieved in the framework of the approximation used.

4.3. *Active transition control*

The effectiveness of the model comprising resonant TS-triads may be demonstrated in an analysis of the experiment by Thomas (1983) on the control of boundary-layer transition using a wave superposition principle. According to Thomas (1983), at two downstream positions x_0 and x_1 ($x_0 < x_1$), two harmonic disturbances of frequency ω_1 were induced into the boundary layer. They may be thought of as waves with complex amplitudes A_1 and $\tilde{A}_1$, respectively. A rapid amplification of quasi-two-dimensional TS-waves with frequency ω_1 was detected in the regimes of individual operation of each vibrator ($b_1 \neq 0$, $\tilde{b}_1 \equiv 0$ and $b_1 \equiv 0$, $\tilde{b}_1 \neq 0$). It was noticed that if $b_1(x_1) = \tilde{b}_1(x_1)$, then the disturbance intensity originating from the second vibrator was much higher in the region $x > x_1$ (figure 19). When both vibrators were in use, and under the conditions ($b_1(x_1) = \tilde{b}_1(x_1)$, $\phi(x_1) \approx \tilde{\phi}(x_1) + \pi$), a sharp reduction in wave intensity was observed in the vicinity of $x \approx x_1$. This was followed by a region of linear development, and then a new rapid growth occurred (figure 19). The explosive character of the amplification, and the intense subharmonical wave ($\omega = \frac{1}{2}\omega_1$) detected in the power spectrum suggests that such amplitude behaviour is the result of nonlinear resonance between induced two-dimensional waves and the three-dimensional background. As a model problem we considered the evolution of two pairs of TS-triads excited at x_0 and x_1. These triads included oblique waves propagating in the direction which corresponds to σ_m. The results are presented in figure 19. Initial values $b_{2,3}(x_0) = 5 \times 10^{-6}$, $\tilde{b}_{2,3}(x_1) = 2 \times 10^{-4}$ were chosen to match the growth of b_1 and $\tilde{b}_1$ in the individual regimes. The difference between initial values $b_2(x_0)$ and $\tilde{b}_2(x_0)$ can be explained, apparently, by the fact that the location $x = x_0$ was situated in the region of rapid attenuation of three-dimensional waves, in contrast with x_1 which was situated in the unstable region. The calculated

resulting wave $|A_1+\tilde{A}_1| = b(x)$ obtained with $\tilde{\phi}(x) = 0.96\pi$, $b = \tilde{b}_1$ displays complete agreement with experimental data. The observed nonlinear growth of $b(x)$ may be explained by the nonlinear influence of three-dimensional waves which were amplified in the interval $x_0 \leqslant x \leqslant x_1$. The efficiency of boundary-layer control was analysed by Zelman & Maslennikova (1987) on the basis of the present model.

5. Higher-order effects

5.1. *Excitation of harmonics*

The resonant interactions considered in the previous section, promote the growth of disturbance intensities. Nonlinear effects of the next order of magnitude then come into play. In the case of controlled experiments, they are related first to two-dimensional wave self-interaction (harmonic generation and mean flow distortion) and non-resonant (two-wave) interaction with subharmonics. An example of numerical results obtained on the basis of equation (2.11) is shown on figure 20. It represents the cross-layer distribution of free-stream velocity for harmonics $u_s = B_s \tilde{u}_s(y)$ with $(\omega_s, \alpha_s, \beta_s) = \{(\frac{3}{2}\omega_1, \alpha_1+\alpha_2, \beta_2), (2\omega_1, 2\alpha_1, 0), (\frac{5}{2}\omega_1, 2\alpha_1+\alpha_2, \beta_2)\}$. The behaviour of B_s and $\tilde{v}_{1s}$ shows a good correlation with experimental data and with data obtained from numerical simulations (Kachanov *et al.* 1984; Fasel, Rist & Konzelman 1987). (Note that according to our calculations, the y-distribution of $\tilde{u}_s(\omega_s = \frac{3}{2}\omega_1)$ can change considerably, depending on downstream position and β/α (figure 20).

5.2. *Analysis of BL- and CNB-models*

Excitation of harmonics can initiate new resonant interactions with the background. In particular, BL-triads can appear. In order to analyse their competitiveness, we considered the TS-wave system ($j = 1, \ldots, 5$) comprising a two-dimensional wave $(\omega_1, \alpha_1, \beta_1 = 0)$ and two symmetrical pairs: $(\omega_{2,3}, \alpha_2 = \alpha_3, \beta_2 = -\beta_3)$ and $(\omega_{4,5} = \alpha_4 = \alpha_5, \beta_4 = \beta_5)$. In this system the waves formed two types of triads: resonant ($j = 1, 2, 3$) and BL ($j = 1, 4, 5$). Amplitude equations for $|A_1| \geqslant |A_j|$ are

$$\left(W_{11}\frac{\mathrm{d}}{\mathrm{d}x} - \gamma_1\right) A_1 = \epsilon S_{1,2+3} h_{1,2+3} A_2 A_3 + \epsilon^2 \{S_{1,(1-1)+1} + S_{1,(1+1)-1}\} |A_1|^2 A + O(\epsilon^2 A_1 A_j^2), \quad (5.1a)$$

$$\left(W_{12}\frac{\mathrm{d}}{\mathrm{d}x} - \gamma_2\right) A_{2,3} = \epsilon S_{2,1-3} h_{2,1-3} A_1^* A_{3,2} + O(\epsilon^2 A_1^2 A_j), \quad (5.1b)$$

$$\left(W_{14}\frac{\mathrm{d}}{\mathrm{d}x} - \gamma_4\right) A_{4,5} = \epsilon^2 \{S_{4,(1+1)-5} + S_{4,(1-5)+1}\} h_{4,(1+1)-5} A_1^2 A_{5,4}^* + \epsilon^2 \{S_{4,(1+1)+4} + S_{4,(1+4)-1}\} |A_1|^2 A_{4,5}. \quad (5.1c)$$

The excitation of $A_{4,5}$ was connected with the nonlinear generation of two- and three-dimensional harmonics ($\sim A_1^2$ and $\sim A_1 A_{4,5}$ respectively) and the mean flow distortion ($\sim |A_1|^2$ and $\sim A_1 A_{5,4}^*$). The model given here may be thought as a generalization of those which considered the effects of wave self-interaction (Zelman & Maslennikova 1984, 1989) or secondary instability in the field of a linear two-dimensional wave (Herbert 1988). Now we shall show that our model can be incorporated into the CNB-model (Nayfeh & Bozatli 1979) which includes a two-dimensional wave A_1 and three-dimensional waves $A_{4,5}$, both with fundamental frequency ω_1, and a two-dimensional

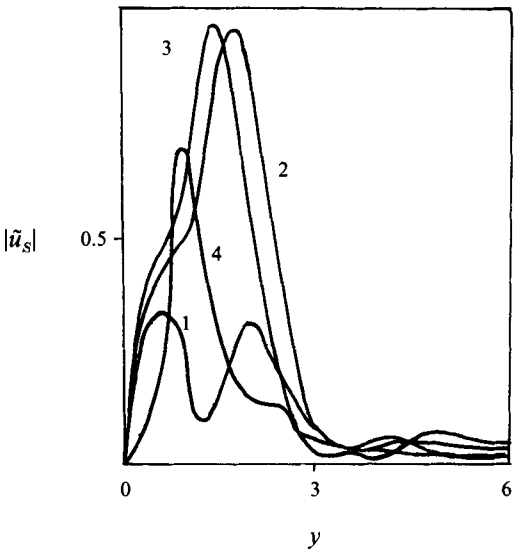

FIGURE 20. Normalized y-distribution of harmonics $\tilde{u}_s$: $\frac{3}{2}\omega_1$ at curve 1, ($Re = 525$, $\beta/\alpha_{\frac{3}{2}} = 0.45$); 2, ($Re = 640$, $\beta/\alpha_{\frac{3}{2}} = 0.64$); 3, ($Re = 755$, $\beta/\alpha_{\frac{3}{2}} = 0.45$). $\frac{5}{2}\omega_1$ at ($Re = 640$, $\beta/\alpha_{\frac{5}{2}} = 0.38$) (curve 4). $F_1 = 110 \times 10^{-6}$.

wave with parameters $(A_0, \omega_0 = 2\omega_1, \alpha_0 = \alpha(2\omega), \beta = 0)$, but $A_{2,3} \equiv 0$. In this case the second-order amplitude equations take the form

$$\left(W_{11}\frac{\mathrm{d}}{\mathrm{d}x} - \gamma_1\right) A_1 = \epsilon S_0 A_0 A_1^* h_{1,0-1}, \tag{5.2a}$$

$$\left(W_{10}\frac{\mathrm{d}}{\mathrm{d}x} - \gamma_0\right) A_0 = \epsilon S_{01} A_4 A_5 \mathrm{e}^{\mathrm{i}\Delta_1} + \epsilon S_{02} A_1^2 h_{1,0-1}, \tag{5.2b}$$

$$\left(W_{14}\frac{\mathrm{d}}{\mathrm{d}x} - \gamma_4\right) A_{4,5} = \epsilon S_{03} A_0 A_{5,4}^* \mathrm{e}^{-\mathrm{i}\Delta_1}, \tag{5.2b}$$

where $\Delta_1 = \int (\alpha_0 - 2\alpha_4)\,\mathrm{d}x$, and S_0, S_{0i} can be calculated according to the general procedure (see §2).

We seek a solution of (5.2) in the form $A_0 = A_{01} + A_{02}$, where A_{01}, A_{02} satisfy (5.2) with $S_{02} \equiv 0$ and $S_{01} \equiv 0$, respectively. Taking into account that the wavenumbers of harmonic and OS eigenvalues for the given $\omega_0 = 2\omega_1$ are quite different: $\Delta = \alpha_0(2\omega_1) - 2\alpha(\omega_1) \gg \epsilon$, $h_{1,0-1} \approx 0$, $\Delta_1 \sim \partial A_0/\partial x\, A_0 \ll \Delta$, and noting the condition $-\gamma_0 \gg |S_{02} A_4 A_5 / A_0|$, realized in the CNB-model (Nayfeh & Bozatli 1979), we obtain the following equations:

$$A_0 \approx \frac{S_{02} A_1^2}{\mathrm{i}\Delta + \gamma_0} = A_{02}, \tag{5.3a}$$

$$\left(W_{11}\frac{\mathrm{d}}{\mathrm{d}x} - \gamma_1\right) A_1 \approx \frac{S_0 S_{02}}{\mathrm{i}\Delta + \gamma_0} A_1^* A_1^2, \tag{5.3b}$$

$$\left(W_{14}\frac{\mathrm{d}}{\mathrm{d}x} - \gamma_4\right) A_{4,5} - \frac{\mathrm{i}}{2} W_{14} \Delta_1 A_{4,5} = \frac{S_{03} S_{02}}{\mathrm{i}\Delta + \gamma_0} A_1^2 A_{5,4}^*. \tag{5.3c}$$

Equations (5.3) describe the resonant interaction between a pair of three-dimensional TS-waves and the second harmonic of the two-dimensional fundamental. Concerning equations (5.1) this effect (modulation instability) is accounted for by the terms

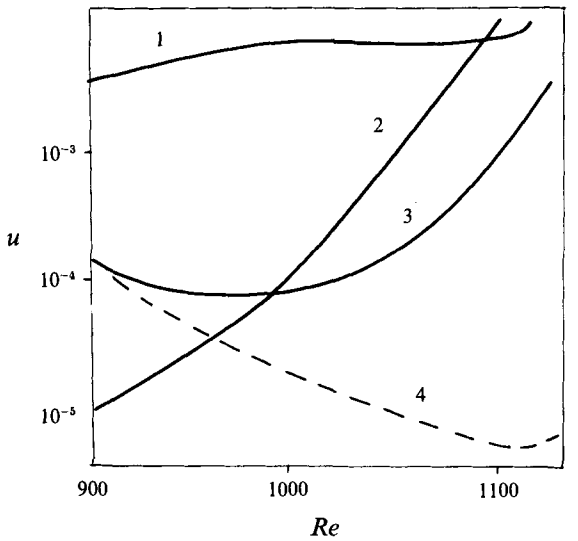

FIGURE 21. Competition of primary and subharmonic resonances. Amplitude growth: curve 1, fundamental; 2, three-dimensional subharmonic; 3, three-dimensional fundamental, $\lambda = 1.6$; 4, three-dimensional fundamental without the v_{1-5} term. $F_1 = 59 \times 10^{-6}$.

proportional to $S_{4,(1+1)-5}$. Numerical results based on equations (5.1) and (5.3) (Zelman & Maslennikova 1984) showed quantitative agreement with results of Nayfeh & Bozatli (1979).

Figure 21 displays typical behaviour obtained from the full system (5.1) (Zelman & Maslennikova 1989). The generation of longitudinal quasi-steady vortices $\sim v_5 A_1 A^*_{5,4}$ was established as the basic mechanism of $A_{4,5}$ amplification (see figure 21). Other types of interaction led to $A_{4,5}$ amplification only in the region of explosive growth of the fundamental wave caused by subharmonic resonance (for $|A_{2,3}| > |A_1|$) or by self-interaction (for $|A_1| > 10^{-2}$, $|\tilde{u}_1 A_1| \geqslant 3 \times 10^{-2}$). In both cases the analysis went beyond the region of applicability of weakly nonlinear theory, as well as of the secondary instability method. The intensity of the longitudinal vortex and the $A_{4,5}$ growth rate depended critically on the detuning parameter $\Delta(\beta, Re, \omega) = \alpha_1 - \alpha_4$, and reached maximum values as $\Delta \to \delta_* \ll 1$.

Local cross-layer distributions of $\tilde{u}_{1-5}(y)$ and corresponding amplification curves for various β/α are shown in figure 22(a, b). It can be seen that subharmonic amplification dominates in the process. Amplification rates for three-dimensional waves in the BL-triad become comparable with those for subharmonics only in the limiting case where weakly nonlinear theory is applicable: $|A_{10}| > 10^{-2}$. The mechanism of nonlinear interactions promotes energy transfer along the spectrum but, in our opinion, is not able to change the type of transition – in particular, to set up K-breakdown in which high-frequency intensities are much higher than low-frequency ones. (For $|A_{10}| \sim 10^{-2}$ and a high background level of fundamentals, the type of transition can be qualified as intermediate.) Keeping in mind the results presented, we may conclude that theories (Craik 1980; Kachanov 1987) based on the weakly nonlinear interaction mechanism are hardly successful in explaining the appearance of K-transition. A sufficient shortcoming of these theories is their lack of explanation for suppression of low-frequency amplification. According to Zelman (1989), this phenomenon can be a result of strong nonlinear distortion of the two-dimensional wave vorticity field in the vicinity of its critical layer, which reduces the parametric growth of background perturbations.

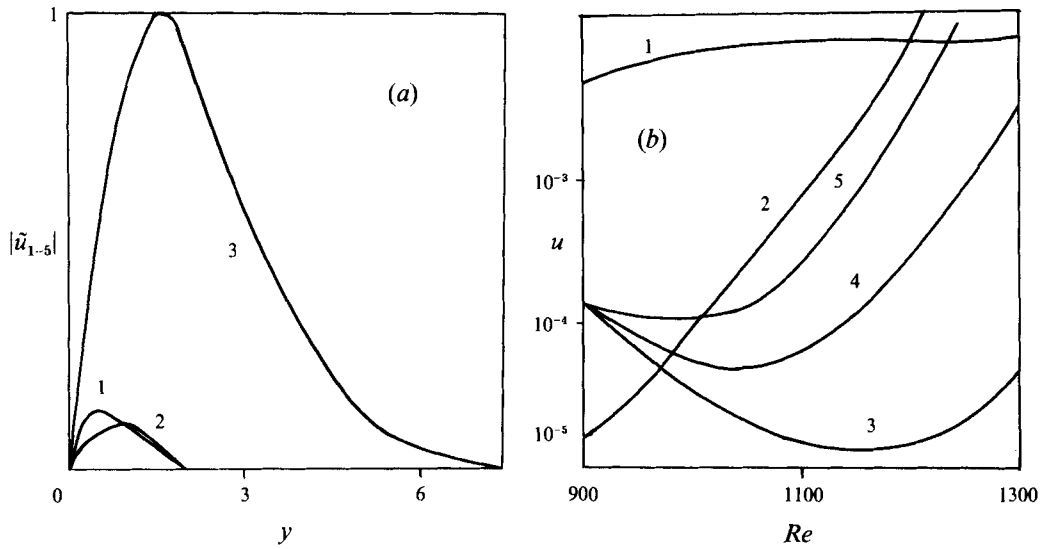

FIGURE 22. (*a*) Normalized local velocity profiles $\tilde{u}_{1-5}$ at $Re = 1120, 1150, 1180$ (curves 1–3); $\lambda = 1.6$. (*b*) Amplitude growth: curve 1, two-dimensional fundamental; 2, three-dimensional subharmonics, $\lambda = 2$; 3–5, three-dimensional fundamental with $\lambda = 1, 1.4, 1.6$ respectively. $F_1 = 59 \times 10^{-6}$.

6. Conclusions

The present investigation revealed S-transition to originate from interaction of TS-waves considered by the first-order weakly nonlinear theory. Interaction of such a kind promotes a selection of dominant structure which was found to be a resonant wave triad comprising one two-dimensional high-frequency and two three-dimensional low-frequency waves. The selectivity can occur through the pre-existing domination in the spectrum of relevant waves, or through the selection of waves according to their growth rates provided the background is homogeneous. In the latter case, which is typical for vibrating ribbon experiments, the dominant structure was revealed to be a symmetrical subharmonic triad. The direction of propagation of the three-dimensional waves (angle structure) turned out to be defined by the initial intensity of the two-dimensional primary wave. Symmetrization (amplitude equalization for the waves propagating to the right and to the left with respect to the downstream direction) arose spontaneously as the waves propagated downstream. The mechanism of amplification of three-dimensional low-frequency waves appeared to be a parametric resonance in the field of the two-dimensional fundamental.

Parametric amplification causes a superexponential growth of three-dimensional wave intensity, and continues up to the stage ($Re = Re_1$) where it exceeds the fundamental wave intensity. Then a nonlinear interaction initiates an explosive growth of all the waves involved. Local amplification rate depends both on the wave parameters and the location (Reynolds number) with respect to the two-dimensional wave neutral stability curve. It should be emphasized that the maximum resonant growth rates generally occur in triads which are far from exact synchronization: $\Delta\theta \neq 0$. The selection of structures with $\Delta\theta = 0$ (C-mechanism) happens at low two-dimensional wave intensity. At the same time the H-mechanism hardly operates, owing to the weak amplification of Squire-mode disturbances and the incompatibility of their y-profiles with experimental data.

Simultaneously with the selection of dominant structure, the three-wave resonant mechanism promotes energy transformation to a broadband spectrum of low-

frequency three-dimensional disturbances. The broadening of the large-scale low-frequency spectrum, being a principal feature of S-transition, can be modelled by a multiwave system comprising interacting TS-waves in which a cascade process occurs. Results achieved permit us to explain some experimental data, and demonstrate good agreement with observations as well as with computer simulations of Navier–Stokes equations in practically all available cases.

Analysis of next-order effects reveals a good correlation between numerically obtained results and experimental data on y-profiles and on growth rates for higher harmonics, and permits us to estimate the competitiveness of resonant and non-resonant BL-triads, which were supposed to be responsible for K-transition. This analysis shows that the CNB-model involves only one type of interaction which takes place in the BL-triad (modulation instability). This instability indeed promotes an amplification of a symmetrical pair of three-dimensional fundamental waves, but this process is much weaker than the interaction of a two-dimensional wave with longitudinal quasi-steady vortices. Nevertheless none of the above effects influences the dominant amplification of the low-frequency component unless initial intensities do not exceed the level of 1% of U_∞. This conclusion remains valid in the case of boundary layers with downstream pressure gradient. We may conclude that the principal feature of the initial stage of S-transition is the preferential growth of three-dimensional low-frequency TS-disturbances determined by a universal resonant interaction mechanism. This type of laminar–turbulent transition seems to be the only one possible in boundary layers with $|A| < 10^{-2}$. (The appearance of a K-type of transition for $|A| > 10^{-2}$ we suppose to be connected with nonlinear redistribution of vorticity in the dominant wave critical layer (Zelman 1989).)

It should be emphasized that the idea of transition as a universal process which includes a long interval of parametric amplification of the background in the field of unstable quasi-linear waves enables us to suggest a rational interpretation of the e^N-method for the definition of the transition location Re_{tr} (Jaffe, Okamura & Smith 1970). Actually, under natural conditions the level of the initial disturbances hardly changes. Then the location of the nonlinear regime $Re \approx Re_n$ is defined by the linear growth rate of the most amplified mode. In Zelman & Maslennikova (1987) a suggestion was made, further supported by experiment (Corke & Mangano 1989), that the saturation of nonlinear explosive growth in triads takes place close to Re_n, in the region where turbulence can be said to have occurred. If this is the case, then $Re_n \approx R_{tr}$. That explains the link between linear amplification of the most unstable wave and the location of transition. This speculation was supported by numerical results on a transitional airfoil (Zelman & Maslennikova 1987). Note, however, that the nature of the primary wave (crossflow instability, Görtler vortices, etc.) is not important.

The authors wish to express thanks to Professor V. Ya. Levchenko and Dr B. V. Smorodsky who have influenced this work by their stimulating discussion.

REFERENCES

BAYLY, B. J., ORSZAG, S. A. & HERBERT, TH. 1988 Instability mechanisms in shear-flow transition. *Ann. Rev. Fluid Mech.* **20**, 359.

BENNEY, D. J. 1964 Finite amplitude effects in an unstable laminar boundary layer. *Phys. Fluids* **7**, 319.

BENNEY, D. J. & LIN, C. C. 1960 On the secondary motion induced by oscillations in a shear flow. *Phys. Fluids* **3**, 656.

BOUTHIER, M. 1973 Stabilité linéaire des écoulements presque parallels. La couche limite de Blasius. *J. Méc.* **72**, 75.

CORKE, T. C. & MANGANO, R. A. 1987 Transition of a boundary layer: controlled fundamental-subharmonic interactions. In *Turbulent Management and Relaminarization, IUTAM Symp. Bangalore, India*, pp. 199–213. Springer.

CORKE, T. C. & MANGANO, R. A. 1989 Resonant growth of three-dimensional modes in transitioning Blasius boundary layers. *J. Fluid Mech.* **209**, 93.

CRAIK, A. D. D. 1971 Nonlinear resonant instability in boundary layers. *J. Fluid Mech.* **50**, 393.

CRAIK, A. D. D. 1980 Nonlinear evolution and breakdown in unstable boundary layers. *J. Fluid Mech.* **99**, 247.

CRAIK, A. D. D. 1985 *Wave Interactions in Fluid Flows.* Cambridge University Press.

FASEL, H. F., RIST, U. & KONZELMAN, U. 1987 Numerical investigation of the three-dimensional development in boundary layer transition. *AIAA Paper* 87-1203.

FISCHER, T. M. & DALLMANN, U. 1991 Primary and secondary stability analysis of a three-dimensional boundary layer. In *Boundary Layer Transition & Control, Cambridge, UK*, pp. 5.1–5.14.

GASTER, M. 1974 On the effect of boundary layer growth on flow stability. *J. Fluid Mech.* **66**, 465.

GASTER, M. 1984 On transition to turbulence in boundary layers. In *Proc. IUTAM Symp. on Turbulence and Chaotic Phenomena in Fluids, Kyoto, Japan*, pp. 99–106. North-Holland.

GOLDSHTIK, M. A., LIFSHITS, A. M. & SHTERN, V. N. 1984 Threshold regimes in the plane channel flow. In *Laminar-Turbulent Transition* (ed. V. Kozlov), pp. 191–198. Springer.

HERBERT, TH. 1983 Secondary instability of plane channel flow to subharmonic three-dimensional disturbances. *Phys. Fluids* **26**, 871.

HERBERT, TH. 1984 Analysis of the subharmonic route to transition in boundary layers. *AIAA Paper* 84-0009.

HERBERT, TH. 1985 Three-dimensional phenomena in transitional flat-plate boundary layer. *AIAA paper* 85-049.

HERBERT, TH. 1988 Secondary instability of boundary layers. *Ann. Rev. Fluid Mech.* **20**, 487.

HERBERT, TH. & BERTOLOTTI, F. 1985 The effects of pressure gradients on the growth of subharmonic disturbances in boundary layers. In *Proc. Conf. Low Reynolds Number Airfoil Aerodyn.* (ed. T. Müller), pp. 65–76. Notre Dame University.

ITOH, N. 1975 Spatial growth of finite wave disturbances in parallel and nearly parallel flows. *Trans. Japan Soc. Aeronaut. Sci.* **17**, 166.

ITOH, N. 1987 Another route to the three-dimensional development of Tollmien–Schlichting waves with finite amplitude. *J. Fluid Mech.* **181**, 1.

JAFFE, N. A., OKAMURA, T. T. & SMITH, A. M. O. 1970 Determination of spatial amplification factors and their application to predicting transition. *AIAA J.* **8**, No. 2, 301.

KACHANOV, YU. S. 1987 On the resonant nature of the breakdown of a laminar boundary layer. *J. Fluid Mech.* **184**, 43.

KACHANOV, YU. S., KOZLOV, V. V. & LEVCHENKO, V. YA. 1977 Nonlinear development of wave in boundary layer. *Izv. Akad. Nauk SSSR, Mech. Zhidk. i Gaza* **3**, 49 (in Russian). (See also *Fluid Dyn.* **12** (1978), 383.)

KACHANOV, YU. S., KOZLOV, V. V., LEVCHENKO, V. YA. & RAMAZANOV, M. P. 1984 On nature of K-breakdown of laminar boundary layer. In *Laminar–Turbulent Transition* (ed. V. Kozlov), pp. 61–74. Springer.

KACHANOV, YU. S. & LEVCHENKO, V. YA. 1982 Resonant interactions of disturbances in transition to turbulence in boundary layer. Preprint N10-82, ITPM SO AN SSSR, Novosibirsk (in Russian).

KACHANOV, YU. S. & LEVCHENKO, V. YA. 1984 The resonant interaction of disturbances at laminar–turbulent transition in a boundary layer. *J. Fluid Mech.* **138**, 209.

KELLY, R. E. 1967 On the stability of an inviscid shear layer which is periodic in space and time. *J. Fluid Mech.* **27**, 657.

KLEBANOFF, P. S. & TIDSTROM, K. D. 1959 Evolution of amplified waves leading to transition in a boundary layer with zero pressure gradient. *NASA Tech. Note* D-195.

KLEBANOFF, P. S., TIDSTROM, K. D. & SARGENT, L. M. 1962 The three-dimensional nature of boundary layer instability. *J. Fluid Mech.* **12**, 1.

KLEISER, L. 1985 Three-dimensional processes in laminar–turbulent transition. In *Nonlinear Dynamics in Transcritical Flows* (ed. H. L. Jordan *et al.*). Lecture Notes in Engineering. Springer.

MASLENNIKOVA, I. I. & ZELMAN, M. B. 1985 On subharmonic-type laminar–turbulent transition in boundary layers. In *Laminar–Turbulent Transition* (ed. V. Kozlov), pp. 21–28. Springer.

MORKOVIN, M. & RESHOTKO, E. 1989 Dialog on progress and issues in stability and transition research. In *Laminar–Turbulent Transition* (ed. D. Arnal & R. Michel), pp. 3–30. Springer.

NAYFEH, A. H. 1987 Nonlinear stability of boundary layers. *AIAA Paper* 87-0044.

NAYFEH, A. H. & BOZATLI, A. N. 1979 Nonlinear interactions in boundary layers. *AIAA Paper* 79-1497.

ORSZAG, S. A. & PATERA, A. T. 1983 Secondary instability of wall-bounded shear flows. *J. Fluid Mech.* **128**, 347.

RAETZ, G. S. 1959 New theory of the cause of transition in fluid flows. *Norair Rep.* NOR 59-383. Howpton, CA.

RIST, U. & FASEL, H. 1991 Spatial three-dimensional numerical simulation of laminar–turbulent transition in a flat-plate boundary layer. In *Proc. Conf. Boundary Layer Transition & Control, Cambridge, UK*, pp. 25.1–25.9.

SARIC, W. S., KOZLOV, V. V. & LEVCHENKO, V. YA. 1984 Forced and unforced subharmonic resonance in boundary layer transition. *AIAA Paper* 84-0007.

SARIC, W. S. & NAYFEH, A. H. 1975 Nonparallel stability of boundary-layer flows. *Phys. Fluids* **18**, 945.

SARIC, W. S. & REYNOLDS, G. A. 1980 Experiments on the stability of nonlinear waves in a boundary layer. In *Laminar–Turbulent Transition* (ed. R. Eppler & H. Fasel), pp. 125–134. Springer.

SARIC, W. S. & THOMAS, A. S. W. 1984 Experiments on the subharmonic route to turbulence in boundary layers. In *Proc. IUTAM Symp. on Turbulence and Chaotic Phenomena in Fluids, Kyoto, Japan*, pp. 117–122. North-Holland.

SINGER, B. A., REED, H. L. & FERZIGER, J. H. 1989 The effects of streamwise vortices on transition in the plane channel. *Phys. Fluids* A **1**, 1960.

SMITH, F. T. & STEWART, P. A. 1987 The resonant-triad nonlinear interaction in boundary layer transition. *J. Fluid Mech.* **179**, 227.

SPALART, PH. & YANG, K. S. 1987 Numerical study of ribbon-induced transition in Blasius flow. *J. Fluid Mech.* **178**, 345.

STUART, J. T. 1960 On the nonlinear mechanics of wave disturbances in stable and unstable parallel flows. Part 1. *J. Fluid Mech.* **9**, 353.

STUART, J. T. 1962 On three-dimensional nonlinear effects in the stability of parallel flows. *Adv. Aero. Sci.* **3–4**, 121.

THOMAS, A. S. W. 1983 The control of boundary-layer transition using a wave-superposition principle. *J. Fluid Mech.* **137**, 233.

THOMAS, A. S. W. & SARIC, W. S. 1981 Harmonic and subharmonic waves during boundary-layer transition. *Bull. Am. Phys. Soc.* **26**, 1252.

USHER, J. R. & CRAIK, A. D. D. 1975 Nonlinear wave interactions in shear flows. Part 2. *J. Fluid Mech.* **70**, 437.

VOLODIN, A. G. & ZELMAN, M. B. 1978 Three-wave resonant interaction of disturbances in boundary layer. *Izv. Akad. Nauk SSSR, Mech. Zhidk. i Gaza*, No. 5, 78 (in Russian).

VOLODIN, A. G. & ZELMAN, M. B. 1981 On the nature of differences in some forms of transition in boundary layers. *AIAA J.* **19**, 950.

WATSON, J. 1960 On the nonlinear mechanics of wave disturbances in stable and unstable parallel flows. Part 2. *J. Fluid Mech.* **9**, 371.

ZELMAN, M. B. 1974 On the nonlinear development of disturbances in parallel flows. *Izv. Sib. Otd. Akad. Nauk SSSR* **13**, 16 (in Russian).

ZELMAN, M. B. 1989 The development of nonlinear disturbances in Blasius boundary layer. In *Models in the Mechanics of Nonhomogeneous Systems* (ed. G. Gadijak), pp. 117–136. Novosibirsk, USSR (in Russian). (See also *Russian J. Theor. Appl. Mech.* 1991, No. 2.)

ZELMAN, M. B. & KAKOTKIN, A. PH. 1982 On the weakly nonlinear stability of nonparallel boundary layers. *Chisl. Met. Mech. Spl. Sred* **13**, No. 3 (in Russian).

ZELMAN, M. B. & MASLENNIKOVA, I. I. 1984 On effects of wave disturbance resonant interaction in boundary layer. *Izv. Akad. Nauk SSSR, Mech. Zhidk. i Gaza*, No. 4, 23.

ZELMAN, M. B. & MASLENNIKOVA, I. I. 1985 Resonant interaction of spatial disturbances in a boundary layer. *J. Appl. Mech. Tech. Phys.* **26** (3), 378.

ZELMAN, M. B. & MASLENNIKOVA, I. I. 1987 On the mechanism of active control of subharmonic transition in boundary layer. *J. Appl. Mech. Tech. Phys.* **28** (1), 25. (See also *Proc. 3rd Asian Cong. Fluid Mechanics, 1987, Tokyo, Japan*, pp. 729–732.)

ZELMAN, M. B. & MASLENNIKOVA, I. I. 1989 On the formation of spatial structure of subharmonic transition in Blasius flow. *Izv. Akad. Nauk SSSR, Mech. Zhidk. i Gaza*, No. 3, 77. (See also in *Laminar–Turbulent Transition* 1990 (ed. D. Arnal & R. Michel), pp. 137–142. Springer.)

ZELMAN, M. B. & MASLENNIKOVA, I. I. 1992 Subharmonic transition spectrum generation in boundary layer. *J. Appl. Mech. Tech. Phys.* **33** (2), 197.

ZELMAN, M. B. & SMORODSKY, B. V. 1988 On the resonant interaction of wave packets in boundary layer. *Izv. Akad. Nauk SSSR, Mech. Zhidk. i Gaze*, No. 6, 67 (in Russian). (See also in *Laminar–Turbulent Transition* 1990 (ed. D. Arnal & R. Michel), pp. 285–290. Springer.)

ZHAO, G.-F. & ZHAO, H. 1988 Weakly nonlinear theory for plane Poiseuille flow. *Appl. Math. Mech.* (English edn) **9**, 617.